

PHOTOCATALYTIC OXIDATION OF BENZENE, TOLUENE,
ETHYLBENZENE AND XYLENES (BTEX) BY TITANIUM DIOXIDE (TiO₂)
CEMENTITIOUS MATERIALS FOR AIR POLLUTION CONTROL

Miss Tanutcha Meechaiyo

A Thesis Submitted in Partial Fulfillment of the Requirements
for the Degree of Master of Science Program in Environmental Management
(Interdisciplinary Program)
Graduate School
Chulalongkorn University
Academic Year 2012

Copyright of Chulalongkorn University

บทคัดย่อและแฟ้มข้อมูลฉบับเต็มของวิทยานิพนธ์ตั้งแต่ปีการศึกษา 2554 ที่ให้บริการในคลังปัญญาจุฬาฯ (CUIR)

เป็นแฟ้มข้อมูลของนิสิตเจ้าของวิทยานิพนธ์ที่ส่งผ่านทางบัณฑิตวิทยาลัย

The abstract and full text of theses from the academic year 2011 in Chulalongkorn University Intellectual Repository (CUIR)
are the thesis authors' files submitted through the Graduate School.

การเร่งปฏิกิริยาแบบใช้แสงสำหรับปฏิกิริยาออกซิเดชันของเบนซีน โทลูอิน เอสทิลเบนซีน
และไซลีน โดยใช้ไทเทเนียมไดออกไซด์ผสมกับซีเมนต์สำหรับการควบคุมมลพิษอากาศ

นางสาวธัญชา มีไชโย

วิทยานิพนธ์นี้เป็นส่วนหนึ่งของการศึกษาตามหลักสูตรปริญญาวิทยาศาสตรมหาบัณฑิต
สาขาวิชาการจัดการสิ่งแวดล้อม (สหสาขาวิชา)
บัณฑิตวิทยาลัย จุฬาลงกรณ์มหาวิทยาลัย
ปีการศึกษา 2555
ลิขสิทธิ์ของจุฬาลงกรณ์มหาวิทยาลัย

Thesis Title PHOTOCATALYTIC OXIDATION OF BENZENE,
TOLUENE, ETHYBENZENE AND XYLENES (BTEX) BY
TITATIUMDIOXIDE (TiO₂) CEMENTITIOUS MATERIALS
FOR AIR POLLUTION CONTROL

By Miss Tanutchai Meechaiyo

Field of Study Environmental Management

Thesis Advisor Professor Say Kee Ong, Ph.D.

Thesis Co-advisor Assistant Professor Tawan Limpiyakorn, Ph.D.

Accepted by the Graduate School, Chulalongkorn University in Partial
Fulfillment of the Requirements for the Master's Degree

..... Dean of the Graduate School
(Associate Professor Amorn Petsom, Ph.D.)

THESIS COMMITTEE

.....Chairman
(Assistant Professor Chantra Tongcumpou, Ph.D.)

.....Thesis advisor
(Professor Say Kee Ong, Ph.D.)

.....Thesis Co-advisor
(Assistant Professor Tawan Limpiyakorn, Ph.D.)

.....Examiner
(Associate Professor Jin Anotai, Ph.D.)

.....External Examiner
(Sorawit Powtongsook, Ph.D.)

รณชชา มีไชโย : การเร่งปฏิกิริยาแบบใช้แสงสำหรับปฏิกิริยาออกซิเดชันของเบนซีน โทลูอีน เอสทิล เบนซีนและไซลีน โดยใช้ไททาเนียมไดออกไซด์ผสมกับซีเมนต์สำหรับการควบคุมมลพิษอากาศ (PHOTOCATALYTIC OXIDATION OF BENZENE, TOLUENE, ETHYBENZENE AND XYLENES (BTEX) BY TITATIUMDIOXIDE (TiO₂) CEMENTITIOUS MATERIALS FOR AIR POLLUTION CONTROL) อ. ที่
 ปรึกษาวิทยานิพนธ์หลัก: Prof. Say Kee Ong, อ. ที่ปรึกษาวิทยานิพนธ์ร่วม: ผศ.ดร.ตะวัน ลิ้มปิยากร,
 90 หน้า

ตัวเร่งปฏิกิริยาแบบใช้แสงที่ถูกผสมเข้าไปในซีเมนต์ได้ถูกประยุกต์ใช้ในพื้นผิวด้านนอกของอาคาร เพื่อใช้สำหรับการทำความสะอาดสิ่งสกปรกด้วยตนเองและการฆ่าเชื้อโรคด้วยตัวเอง เมื่อไม่นานมานี้ ตัวเร่งปฏิกิริยาแบบใช้แสง เช่น ไททาเนียมไดออกไซด์ได้ถูกใช้ผสมในซีเมนต์ที่เอาไว้ใช้ในการทำถนน ซึ่งนับว่าเป็นเทคโนโลยีนวัตกรรมใหม่ที่ถูกใช้ในการควบคุมมลพิษที่เกิดมาจากการใช้รถใช้ถนน แต่อย่างไรก็ตาม ในขณะนี้ยังมีข้อมูลไม่มากเกี่ยวกับการนำไปใช้ปฏิบัติของไททาเนียมไดออกไซด์ที่ผสมกับซีเมนต์ในการทำถนนสำหรับการกำจัดสารจำพวกไฮโดรคาร์บอน ในการศึกษานี้จะศึกษาการย่อยสลายของเบนซีน โทลูอีน เอสทิลเบนซีน และไซลีน (BTEX) ในอากาศโดยใช้แผ่นปูนหนาที่ผสมไททาเนียมไดออกไซด์เข้าไปและการทดลองนี้จะทำการทดลองโดยใช้เครื่องปฏิกรณ์ในห้องปฏิบัติการ ตัวแปรทางด้านสิ่งแวดล้อมที่จะทำการศึกษา ได้แก่ ความชื้นสัมพัทธ์ อัตราการหมุนเวียนของปริมาณอากาศ อายุของแผ่นปูนหนา และความเข้มของแสงอัลตราไวโอเล็ต ตัวอย่างของอากาศทั้งด้านเข้าและด้านออกจะถูกวิเคราะห์ความเข้มข้นของสารแต่ละตัวโดยใช้แก๊สโครมาโตกราฟีแบบใช้พลังงานจากโฟตอนในการแยกสลาย (Gas chromatography with photoionization detector)

จากการทดลองพบว่า ค่าความชื้นสัมพัทธ์ที่ 50 % เป็นค่าเหมาะสมในการกำจัดสารมลพิษ โดยที่การลดลงของการกำจัดมลสารจะเกิดขึ้นเมื่อมีความต่ำหรือสูงเกินไปของความชื้นสัมพัทธ์ ในขณะที่เปอร์เซ็นต์สารกลุ่มบีเทกถูกค้นพบว่า เมื่อเพิ่มอัตราเร็วของอากาศความสามารถในการกำจัดสารกลุ่มบีเทกจะลดลง แต่ว่ามวลที่ถูกกำจัดออกไปจะเพิ่มขึ้นเมื่อเพิ่มอัตราเร็วของอากาศ ในทางเดียวกันเมื่อเพิ่มความเข้มข้นของแสงอัลตราไวโอเล็ตจาก 5-12 วัตต์ต่อลูกบาศก์เมตร จะส่งผลให้เป็นการเพิ่มขึ้นของมวลที่ถูกกำจัดทิ้ง จะกล่าวได้ว่าไททาเนียมไดออกไซด์ที่ถูกผสมในซีเมนต์สามารถประยุกต์ใช้เป็นหนึ่งในเทคโนโลยีที่ใช้ในการบรรเทาปัญหามลพิษอากาศ

สาขาวิชา การจัดการสิ่งแวดล้อม.....ลายมือชื่อนิสิต.....
 ปีการศึกษา 2555.....ลายมือชื่อ อ.ที่ปรึกษาวิทยานิพนธ์หลัก.....
 ลายมือชื่อ อ.ที่ปรึกษาวิทยานิพนธ์ร่วม.....

5487535620 : MAJOR ENVIRONMENTAL MANAGEMENT

KEYWORDS : TiO₂ / PHOTOCATALYTIC OXIDATION / BTEX / AIR
POLLUTION / CEMENTITIOUS MATERIALS

TANUTCHA MEECHAIYO : PHOTOCATALYTIC OXIDATION OF
BENZENE, TOLUENE, ETHYLBENZENE AND XYLENES (BTEX) BY
TITANIUM DIOXIDE (TiO₂) CEMENTITIOUS MATERIALS FOR AIR
POLLUTION CONTROL. ADVISOR: PROF. SAY KEE ONG, Ph.D., CO-
ADVISOR: ASST. PROF. TAWAN LIMPIYAKORN, Ph.D., 90 pp.

Cementitious materials with active photocatalytic agents have been applied on external surfaces of buildings for self cleaning and self-disinfecting purposes. Recently, active photocatalytic agents such as TiO₂ have been used in road pavement concrete as an innovative technology for the control of roadside air pollution. There is currently not much information available on the implementation of TiO₂ active pavements for the removal of hydrocarbon pollution. In this study, degradation of benzene, toluene, ethylbenzene and xylene (BTEX) in air by TiO₂ active concrete slabs were investigated in a laboratory-scale reactor. Environmental variables studied included relative humidity (RH), air flow rate, aging and UV intensity. BTEX concentrations in inlet and outlet air samples were analyzed using a gas chromatograph with photoionization detector.

The optimal RH for BTEX mass removal was approximately 50% with decreasing mass removal for lower or higher RH. Percent removals of BTEX were found to decrease with higher flow rate but mass removed increased with air flow rate. Similarly, an increase in UV intensity from 5 to 12 W/m² resulted in an increase in mass removal. Overall, it appeared that TiO₂ active materials may be used as a passive technology in mitigating air pollution from motor vehicles.

Field of Study: Environmental Management Student's Signature.....
Academic Year: 2012 Advisor's Signature.....
Co-advisor's Signature.....

ACKNOWLEDGEMENTS

This thesis would not have been possible without the kind support of many people, who always supported me from the initial to the final stage.

First of all, I would like to express my heartfelt gratitude to my advisor, Prof. Say Kee Ong for his patience, wise guidance and valuable help, and for sharing his knowledge and skills throughout my study. I would like to thank my co-advisor, Assistant Professor Dr. Tawan Limpiyakorn for his advice regarding my work and his kind support. In addition, I gratefully acknowledge the support of my thesis chairman, Asst. Prof. Chantra Tongcumpou, and committee members, Assoc. Prof. Jin Anotai, and Dr. Sorawit Powtongsook and for their stimulating questions and valuable suggestions.

I particularly would like to thank Mr. Joel Sikkema (Ph.D. student) for his assistance in the experimental setup, kind help during my times in the laboratory and Ames, and teaching me the Minitab software. I appreciate the support of Mr. Ben Bai (Master student), Ms. Navaporn Kanjanasiranont (Ph.D. student) and Ms. Pitchaya Patanaanake (Master student) for suggestions and valuable advices.

I would like to express my profound gratitude to the Center of Excellence for Environmental and Hazardous Waste Management (EHWM), Chulalongkorn University, for granting me support to pursue my graduate studies and to work on a thesis of my interest.

Finally and most importantly, I am extremely grateful for the support of my parents and family who are my inspiration for living and doing everything. Their love and warm encouragement have been my greatest strength and inspiration for my success in the past, now, and in the future.

CONTENTS

	Page
ABSTRACT IN THAI	iv
ABSTRACT IN ENGLISH	v
ACKNOWLEDGEMENTS	vi
CONTENTS	vii
LIST OF TABLES	x
LIST OF FIGURES	xii
LIST OF ABBREVIATIONS	xvi
CHAPTER I INTRODUCTION	1
1.1 Background.....	1
1.2 Objective.....	2
1.3 Hypotheses.....	2
1.4 Scope of the Study	3
CHAPTER II LITERATURE REVIEW	4
2.1 Introduction.....	4
2.2 Principle of Titanium Dioxide (TiO ₂) Photocatalysis.....	6
2.2.1 Background of Titanium dioxide.....	6
2.2.2 Reactions of TiO ₂	8
2.2.3 TiO ₂ - based building materials.....	10
2.2.4 Parameter impacting on Photocatalytic Efficiency.....	11
2.2.5 Data gaps and research questions about TiO ₂ photocatalytic oxidation....	14
2.3 Air Purification to Eliminate Nitrogen Oxide (NO _x).....	16
2.3.1 Background, qualification and toxicity.....	16
2.3.2 Current work to eliminate Nitrogen oxide (NO _x).....	16
2.4 Air Purification to Eliminate Volatile Organic Compounds (VOCs).....	19

	Page
2.4.1. Background, qualification and toxicity	19
2.4.2. Current work to eliminate VOCs.....	21
CHAPTER III METHODOLOGY.....	24
3.1 Materials and Apparatus.....	24
3.1.1 Chemicals	24
3.1.2 Instruments and laboratory-slabs.....	24
3.2 Experimental Procedures.....	26
3.2.1 Preparation of photocatalytic concrete slabs.....	26
3.2.2 Laboratory setup.....	28
3.2.3 Analytical method.....	32
3.2.4 Operational procedure.....	32
CHAPTER IV RESULTS AND DISSCUSION.....	34
4.1 Photocatalytic Degradation of BTEX.....	34
4.2 Effect of relative humidity on BTEX degradation	35
4.3 Effect of flow rate on BTEX degradation	38
4.4 Effect of intensity on BTEX degradation.....	41
4.5 Effect of aging on BTEX degradation	44
CHAPTER V CONCLUSIONS AND RECOMMEDATIONS.....	46
5.1 Conclusions.....	46
5.2 Recommendations for Future Work.....	47
REFERENCES.....	48

	Page
APPENDICES	58
APPENDIX A.....	59
APPENDIX B.....	70
BIOGRAPHY	90

LIST OF TABLES

	Page
Table 2.1 Basic physical-chemical properties of TiO ₂	7
Table 2.2 Impact of environmental parameters on the rate of NO _x degradation	20
Table 2.3 Impact of environmental parameters on the rate of BTEX.....	22
Table 3.1 Environmental parameters used in the study.....	31
Table 3.2 Experimental matrix for lab- scale photoreactor tests.....	31
Table A.1 Calibration curve data of Benzene humidity set.....	60
Table A.2 Calibration curve data of Toluene humidity set.....	60
Table A.3 Calibration curve data of Ethylbenzene humidity set.....	61
Table A.4 Calibration curve data of m-Xylene humidity set.....	61
Table A.5 Calibration curve data of o and p-Xylene humidity set.....	62
Table A.6 Calibration curve data of Benzene for flow rate set.....	63
Table A.7 Calibration curve data of Toluene for flow rate set.....	63
Table A.8 Calibration curve data of Ethylbenzene for flow rate set.....	64
Table A.9 Calibration curve data of m-Xylene for flow rate set.....	65
Table A.10 Calibration curve data of o and p-Xylene for flow rate set.....	65
Table A.11 Calibration curve data of Benzene for intensity and aging set.....	66
Table A.12 Calibration curve data of Toluene for intensity and aging set.....	67
Table A.13 Calibration curve data of Ethylbenzene for intensity and aging set.....	67
Table A.14 Calibration curve data of m-Xylene for intensity and aging set.....	68
Table A.15 Calibration curve data of o and p-Xylene for intensity and aging set.....	69
Table B.1 Control experiment for No-TiO ₂ and No-UV at Q=3 L/min, RH=10%, I=10 W/m ²	74

	Page
Table B.2 Mass removed of BTEX at Q=3 L/min, RH=10%, I=10 W/m ²	75
Table B.3 Mass removed of BTEX at Q=3 L/min, RH=25%, I=10 W/m ²	77
Table B.4 Mass removed of BTEX at Q=3 L/min, RH=50%, I=10 W/m ²	78
Table B.5 Mass removed of BTEX at Q=3 L/min, RH=70%, I=10 W/m ²	80
Table B.6 Mass removed of BTEX at Q=1 L/min, RH=50%, I=10 W/m ²	81
Table B.7 Mass removed of BTEX at Q=5 L/min, RH=50%, I=10 W/m ²	83
Table B.8 Mass removed of BTEX at Q=3 L/min, RH=50%, I=5 W/m ²	84
Table B.9 Mass removed of BTEX at Q=3 L/min, RH=50%, I=12 W/m ²	86
Table B.10 Mass removed of BTEX at Q=3 L/min, RH=10%, I=10 W/m ² , 1 month...	87
Table B.11 Mass removed of BTEX at Q=3 L/min, RH=50%, I=10 W/m ² , 3 months..	89
Table B.12 Percent removal of Benzene at different flow rate.....	89
Table B.13 Percent removal of Toluene at different flow rate.....	89

LIST OF FIGURES

	Page
Figure 2.1 Sources of air emissions.....	4
Figure 2.2 The main air pollution in the U.S.	5
Figure 2.3 Mobile source air pollutants.....	5
Figure 2.4 Different crystalline structures of TiO ₂	8
Figure 2.5 Band gaps and Valance band and Conduction band of common semiconductors and standard redox potentials.....	8
Figure 2.6 Photocatalysis and reaction mechanisms of TiO ₂	10
Figure 3.1 Traceable hygrometer and UV radiometer.....	25
Figure 3.2 Mass flow controller and Black Light Blue (BLB) fluorescent lamps 15 W UV-A illumination.....	25
Figure 3.3 Headspace vials and aluminum seal with septa and Crimp.....	26
Figure 3.4 Typical concrete slab for laboratory-scale testing.....	27
Figure 3.5 Method for making TiO ₂ -based concrete slabs.....	27
Figure 3.6 Schematic diagram of experimental apparatus.....	29
Figure 3.7 The experiment setup in the laboratory at department of Civil, Construction and Environmental Engineering, Iowa State University, USA, 2012.....	30
Figure 3.8 10 ppmv BTEX gas mixture using for the experiment.....	30
Figure 3.9 One mL syringe and Tracor 540 gas Chromatography.....	32
Figure 3.10 Running the experiment while turning on the UV light source.....	33
Figure 4.1 The Control experiment for non-TX active cement (no TiO ₂) and non- UV light.....	34
Figure 4.2 Mass of BTEX removal for different relative humidities.....	36
Figure 4.3 Overall Mass removed of BTEX for different relative humidities.....	37

	Page
Figure 4.4 Percent removal and mass removed of benzene (a and c) and toluene (b and d) for different flow rates.....	39
Figure 4.5 Overall Mass removed of BTEX for different relative humidities.....	40
Figure 4.6 Mass of BTEX removed for different intensities.....	42
Figure 4.7 Overall Mass removed of BTEX for different intensities.....	43
Figure 4.8 Mass for BTEX removed for slab at different times after preparation.....	45
Figure A.1 Calibration curve of Benzene for RH set.....	60
Figure A.2 Calibration curve of Toluene for RH set.....	61
Figure A.3 Calibration curve of Ethylbenzene for RH set.....	61
Figure A.4 Calibration curve of m-Xylene for RH set.....	62
Figure A.5 Calibration curve of o and p-Xylene for RH set.....	62
Figure A.6 Calibration curve of Benzene for flow rate set.....	63
Figure A.7 Calibration curve of Toluene for flow rate set.....	64
Figure A.8 Calibration curve of Ethylbenzene for flow rate set.....	64
Figure A.9 Calibration curve of m-Xylene for flow rate set.....	65
Figure A.10 Calibration curve of o and p-Xylene for flow rate set.....	66
Figure A.11 Calibration curve data of Benzene for intensity and aging set.....	66
Figure A.12 Calibration curve data of Toluene for intensity and aging set.....	67
Figure A.13 Calibration curve data of Ethylbenzene for intensity and aging set.....	68
Figure A.14 Calibration curve data of m-Xylene for intensity and aging set.....	68
Figure A.15 Calibration curve data of o and p -Xylene for intensity and aging set.....	69
Figure B.1 Chromatogram for control experiment in the bypass mode without TiO ₂ ...	72
Figure B.2 Chromatogram for control experiment in the photoreactor mode without TiO ₂	72

	Page
Figure B.3 Chromatogram for control experiment in the bypass mode without U...	73
Figure B.4 Chromatogram for control experiment in the photoreactor mode without UV.....	73
Figure B.5 Chromatogram of BTEX at Q=3 L/min, RH=10%, I=10 W/m ² in the bypass mode.....	74
Figure B.6 Chromatogram of BTEX at Q=3 L/min, RH=10%, I=10 W/m ² in the photoreactor mode.....	75
Figure B.7 Chromatogram of BTEX at Q=3 L/min, RH=25%, I=10 W/m ² in the bypass mode.....	76
Figure B.8 Chromatogram of BTEX at Q=3 L/min, RH=25%, I=10 W/m ² in the photoreactor mode.....	76
Figure B.9 Chromatogram of BTEX at Q=3 L/min, RH=50%, I=10 W/m ² in the bypass mode.....	77
Figure B.10 Chromatogram of BTEX at Q=3 L/min, RH=50%, I=10 W/m ² in the photoreactor mode.....	78
Figure B.11 Chromatogram of BTEX at Q=3 L/min, RH=70%, I=10 W/m ² in the bypass mode.....	79
Figure B.12 Chromatogram of BTEX at Q=3 L/min, RH=70%, I=10 W/m ² in the photoreactor mode.....	79
Figure B.13 Chromatogram of BTEX at Q=1 L/min, RH=50%, I=10 W/m ² in the bypass mode.....	80
Figure B.14 Chromatogram of BTEX at Q=1 L/min, RH=50%, I=10 W/m ² in the photoreactor mode.....	81
Figure B.15 Chromatogram of BTEX at Q=5 L/min, RH=50%, I=10 W/m ² in the bypass mode.....	82
Figure B.16 Chromatogram of BTEX at Q=5 L/min, RH=50%, I=10 W/m ² in the photoreactor mode.....	82

	Page
Figure B.17 Chromatogram of BTEX at $Q=3$ L/min, $RH=50\%$, $I=5$ W/m ² in the bypass mode.....	83
Figure B.18 Chromatogram of BTEX at $Q=3$ L/min, $RH=50\%$, $I=5$ W/m ² in the photoreactor mode.....	84
Figure B.19 Chromatogram of BTEX at $Q=3$ L/min, $RH=50\%$, $I=12$ W/m ² in the bypass mode.....	85
Figure B.20 Chromatogram of BTEX at $Q=3$ L/min, $RH=50\%$, $I=12$ W/m ² in the photoreactor mode.....	85
Figure B.21 Chromatogram of BTEX at $Q=3$ L/min, $RH=50\%$, $I=10$ W/m ² in the bypass mode for 1 month aging.....	86
Figure B.22 Chromatogram of BTEX at $Q=3$ L/min, $RH=50\%$, $I=10$ W/m ² in the photoreactor mode for 1 month aging.....	87
Figure B.23 Chromatogram of BTEX at $Q=3$ L/min, $RH=50\%$, $I=10$ W/m ² in the bypass mode for 3 month aging.....	88
Figure B.24 Chromatogram of BTEX at $Q=3$ L/min, $RH=50\%$, $I=10$ W/m ² in the photoreactor mode for 3 month aging.....	88

LIST OF ABBREVIATIONS

EPA	Environmental Protection Agency
CO	Carbon Monoxide
CO ₂	Carbon dioxide
NO _x	Nitrogen Oxides
NO	Nitric Oxide
NO ₂	Nitrogen Dioxide
BTEX	benzene, toluene, ethylbenzene and xylenes
VOCs	Volatile Organic Compounds
TiO ₂	Titanium Dioxide
H ₂ O	Water
TCE	Trichloroethylene
RH	Relative Humidity
Q	Flow Rate
I	Intensity
UV	Ultraviolet
Re	Reynolds number
GC/PID	Gas Chromatography Photoionization Detector
MoDOT	Missouri Department of Transportation
VB	Valence Band
CB	Conduction Band
PCO	Photocatalytic Oxidation
IARC	International Agency for Research on Cancer
WHO	World Health Organization

PMMA	Polymethyl Methacrylate
ASTM	American Society Testing and Materials
BLB	Black Light Blue
Fig.	Figure
US	United States
ISO	International Organization for Standardization
JIS	Japanese Industrial Standard
PICADA Assessment	Photocatalytic Innovative Coverings Applications for Depollution
Kg /m ³	Kilogram per cubic meter
mm ²	Square Millimeter
m	meter
mm	millimeters
nm	nanometer
m ²	square meter
m ³	cubic meter
W	watt
W/ m ²	watt per square meter
mW/cm ²	milliwatt per square centimeter
μW/cm ²	microwatt per square centimeter
ppmv	Parts per million by volume
ft	feet
cft	cubic feet per unit time
L _d	Length
mL	milliliter
mL/min	milliliter per minute

$^{\circ}\text{C}$	degree Celsius
L/min	liter per minute
mol/s g	mole per second gram
m^2/s	square meter per second

CHAPTER I

INTRODUCTION

1.1 Background

It is becoming increasingly difficult to ignore air pollution as one of the more serious environmental problems in the cities especially in developing countries. The United States Environmental Protection Agency (US EPA) reported that the two worst air pollution problems are urban air quality and indoor air pollution with 52% and 27% of the air pollution from industrial and transportation, respectively. Emissions from motor traffic are a very important source of urban air pollution throughout the world. In addition, US EPA indicated that pollution from highway construction can similarly impact the air quality. A study by Kuhns et al. (2004) pointed out that roadside air pollution contributed about 29%, 35% and 58% of the total volatile organic compounds (VOCs), total nitrogen oxides (NO_x), and total carbon monoxide (CO) emitted, respectively in the US. Recent evidence suggests that these concentrations are often higher in cities where urban development and increased traffic volumes add to the emissions; while street canyon conditions inhibit dispersion and mixing, resulting in high ground level concentrations which often exceeded the concentrations of industrial sources (Chen et al., 2008).

According to Thoma et al. (2008), more than 35 million people in the US live close to roads. These people are exposed to transportation pollution and many exhibit varying levels of health effects that are generally associated with NO_x and VOCs. In Thailand, emission loads from mobile sources for NO_x and VOCs were 264,648 and 232,973 tons/year, respectively, while NO_x and VOCs from gasoline generated were about 35,886 tons (15.4%) and 34,133 tons (12.9%), respectively (PCD, 1997). To mitigate air pollution, several efforts are being applied including source reduction and treatment controls. A recent technology being implemented is the use of heterogeneous photocatalytic materials on the building surface. Photocatalytic compounds such as titanium dioxide (TiO₂), which can degrade organic and inorganic pollutants in the air, may eliminate harmful air pollutants such as NO_x and VOCs in the presence of ultraviolet (UV) light (Cassar, 2004). Several studies have shown that

surfaces coated with TiO_2 can be self-cleaning (Fujishima and Zhang, 2006). Recently TiO_2 concrete pavement, made by mixing of Portland cement and TiO_2 , has been proposed as a substitute substrate for air remediation through heterogeneous photocatalytic degradation of air pollutants (Ruot et al., 2009).

The potential of photocatalytic cementitious materials for pavement roads have been demonstrated in a number of laboratory research with NO_x as the pollutants. There are very few studies assessing the TiO_2 concrete for VOCs removal. There is a need to further understand the impact of TiO_2 on air quality. Furthermore, there are very few studies investigating the loss of catalytic activity due to aging of concrete. However, experimental data reported thus far are rather mixed, and there are no general agreements on the effect of each variable on the photocatalytic reaction of the TiO_2 cement. Moreover, not much is known about the intermediate and by products generated from these reactions (Mo et al., 2009)

This research investigates the application of TiO_2 concrete, as an innovative technology and approach, for the heterogeneous photocatalytic degradation of benzene, toluene, ethylbenzene and xylene (BTEX). Experiments will be conducted in a laboratory-scale reactor with concrete slabs containing TiO_2 . Variables to be studied include BTEX concentrations, relative humidity (RH), flow rate (Q), UV intensity (I) and aging of TiO_2 concrete slab.

1.2 Objective

The objective of this research is to investigate the application of TiO_2 -based concrete pavement for the photocatalytic degradation of BTEX in the air under different environment conditions.

1.3 Hypotheses

When exposed to UV light, TiO_2 -based concrete pavements are effective in oxidizing BTEX and the amount of BTEX degraded are dependent on the environmental conditions.

1.4 Scope of the study

1.Experiments were conducted in a laboratory-scale photo reactor where various environmental conditions (BTEX concentrations, relative humidity, intensity, air flow rate) can be varied.

2.Experimental method was adapted from ISO 22197-1: Test method for air purification performance of semiconducting photocatalytic materials -Part 1: Removal of nitric oxide.

3.TiO₂-based concrete slabs were prepared based on the concrete mix design provided by Missouri Department of Transportation (MoDOT).

4.Concentration of BTEX was analyzed using a Gas Chromatograph with a Photoionization Detector (GC/PID).

CHAPTER II

LITERATURE REVIEWS

2.1 Introduction

Air pollution, in urban areas, is one of the more important environmental issues that need to be addressed (Ishihara et al., 2010) to minimize health problems. Exposure to high levels of air pollutants may result in irritation of throats and eyes, or breathing difficulties (Cocheo et al., 2011). Long-term exposure to air pollution may cause damage to the immune, neurological, and respiratory systems and in extreme cases, may even cause death (Schwartz, 2011). There are several sources of air pollutions as shown in Fig.2.1 with the major emission sources from industry (52%) and transportation (27%).

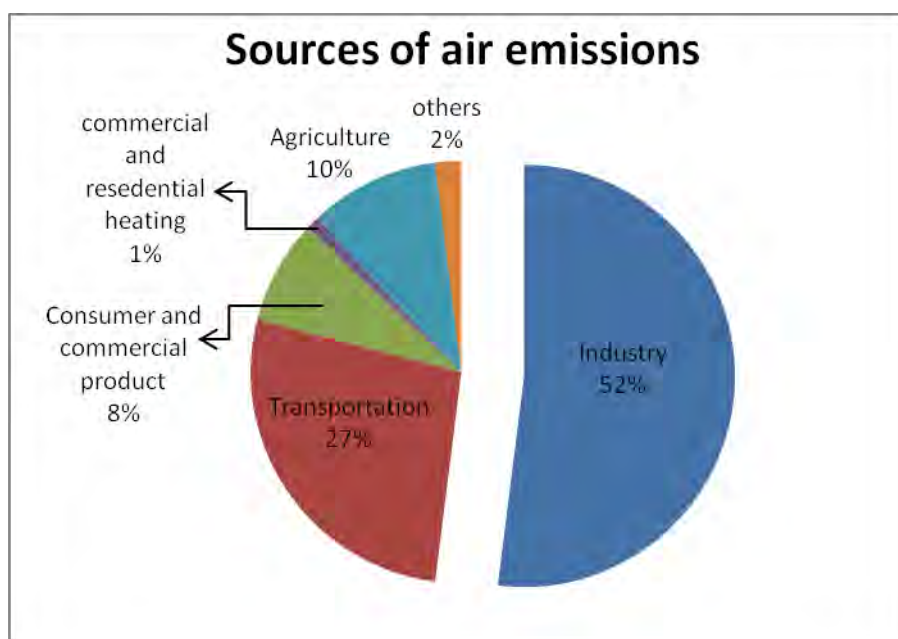


Figure 2.1 Sources of air emissions (Source: Environment Canada, 2002)

A significant source of urban air pollution is emissions from transportation systems which include any air pollution that is emitted by motor vehicles, engines, airplanes and equipment that moves from one location to another (Sawyer et al., 2000). The main pollutants emitted by vehicles are carbon monoxide (CO), oxides of nitrogen (NO_x), volatile organic compounds (VOCs) and particulates as shown in Fig. 2.2. Figure 2.3 shows the main

sources of NO_x and VOCs in the US. Emissions from road vehicles, one of the main sources of NO_x and VOCs, contribute about 30% and 29% of NO_x and VOCs, respectively.

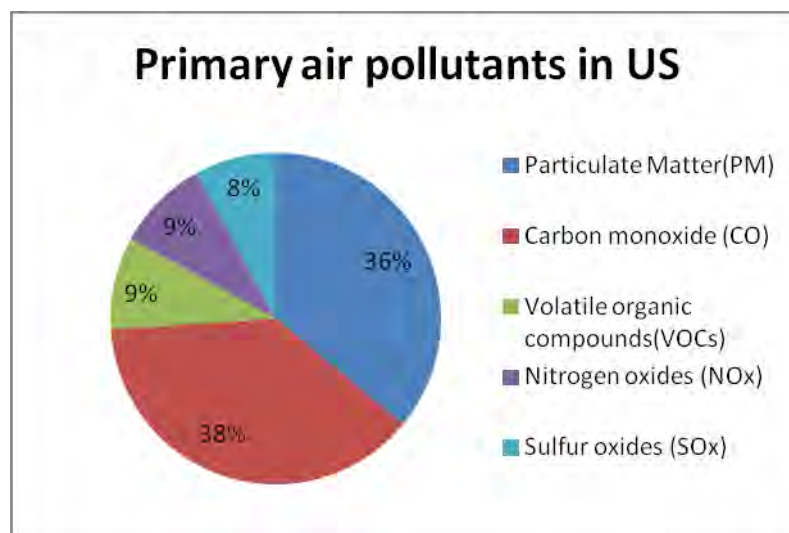


Figure 2.2 Main air pollution in the U.S. (Source: EPA, 2010)

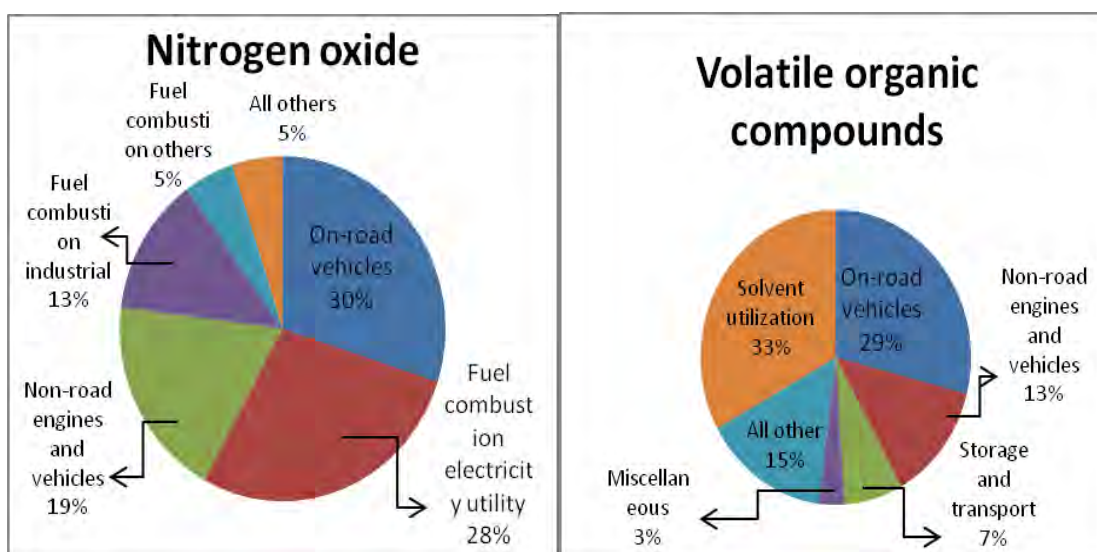


Figure 2.3 Mobile source air pollutants (Source: Christopherson, 2000)

Air pollution is further amplified when NO_2 and volatile organic compounds (VOCs) from motor vehicles react photocatalytically in the presence of sunlight to form ozone, a secondary long-range pollutant (Calvert, 1994). Another impact of NO_2 is the generation of acid rain.

In many countries, mobile sources may be one of the largest contributors of pollutants that are known or suspected to cause cancer or serious respiratory health problems. For example, incomplete combustion of gasoline and diesel may result in emission of benzene, a known human carcinogen (Johnson et al., 2009), and formaldehyde, acetaldehyde, 1,3-butadiene and diesel particulate matter which are probable human carcinogens (Kirman and Grant, 2012). Mobile sources of air toxics have been estimated to account for as much as half of all cancer cases that are attributed to outdoor sources of air toxics (EPA, 1995). However, the number of vehicles on the road and the distance travelled continue to grow which would mean that new and advanced technologies will be required to maintain or reduce the amount of toxic compounds in the environment. Air pollution can be mitigated by reducing emissions from the sources and/or by removing the air pollutants present in the air. One of the innovative approaches currently used in removing air pollution from air is to use surfaces that are coated with chemically-reactive compounds such as photocatalysts.

2.2 Principle of Titanium Dioxide (TiO₂) Photocatalysis

2.2.1 Background of titanium dioxide

Among the many photocatalysts, TiO₂ is an excellent photocatalyst with diverse applications in water and air pollution control to treat various organic pollutants. There are more than 2000 companies worldwide selling air purification products that incorporate TiO₂ materials (Cassar, 2004). The wide usage of TiO₂ is due to its high chemical stability in acidic and basic conditions, nontoxicity, and the relatively low cost and high photocatalytic activity in comparison to other metal oxide photocatalysts. TiO₂ can be mixed with concrete with minimal change in its performance and effectiveness. Under weak solar irradiation, TiO₂ can decompose various air pollutants such as hydrocarbons (Wu et al., 2007), aldehyde (Dechakiatkrai et al., 2007), halogenated compounds (Hung et al., 2007), nitrogen-containing compounds (Alberici et al., 2001), sulfur-containing compounds (Portela et al., 2007) and inorganic compounds at low concentrations (Ao et al., 2003; Wang et al., 2007; Zhang et al., 2003).

Table 2.1 shows the basic physical-chemical properties of TiO₂. TiO₂ exists in three different structures: anatase (tetragonal), brookite (orthorhombic) and rutile (tetragonal). Anatase shows the highest photoactivity of the three structures due to its higher surface density of active sites for adsorption and photocatalysis (Zhao and Yang, 2003) while rutile is the most thermodynamically stable of the three structures. Anatase and brookite are metastable and transform to rutile by heating (Debabrata and Shimanti, 2005). The band gap energies for anatase and rutile have been estimated to be 3.2 and 3.0 eV, respectively, which is the band gap energy of anatase corresponding to photons with a wavelength of 388 nm (wavelength of UV light range between 300-400 nm). Anatase is currently commercially available as thin, transparent films that can be used to coat glass, tiles, and other materials (Berdahl and Akbari, 2008). Overall, the efficient oxidizing effect and qualification of TiO₂ makes it proper for the degradation of organic and inorganic compounds at low concentrations and Fig. 2.4 and 2.5 show different crystalline structures of TiO₂ and band gaps, valence bands and conduction bands of common semiconductors and standard redox potentials respectively.

Table 2.1 Basic physical-chemical properties of titanium dioxide (TiO₂)
(Source: Akimoto, 1994; Winkler and Jochen, 2003)

Properties	Values
Molecular formula	TiO ₂
Molar mass	79.866 g/mol
Appearance	White solid
Odor	Odorless
Density	4.23 g/cm ³
Melting point	1843 °C
Boiling point	2972 °C
Solubility in water	Insoluble

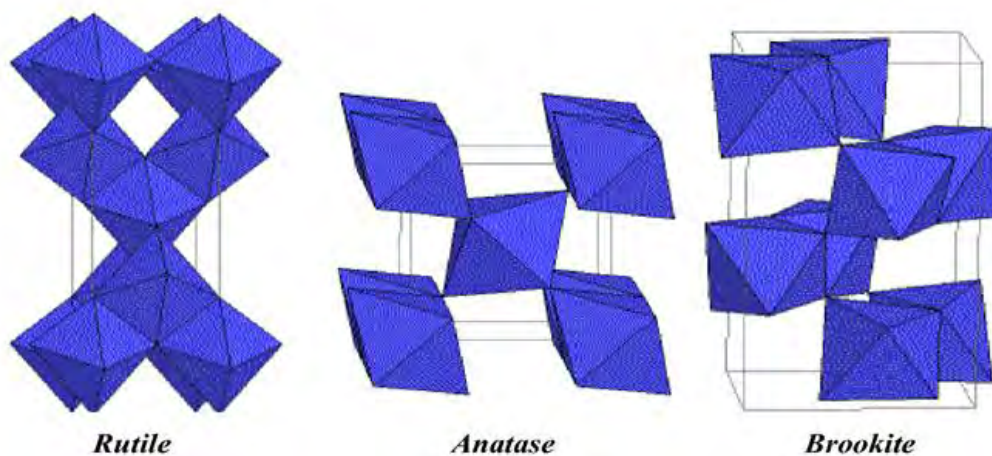


Figure 2.4 Different crystalline structures of TiO_2 (Simons and Dachille, 1967)

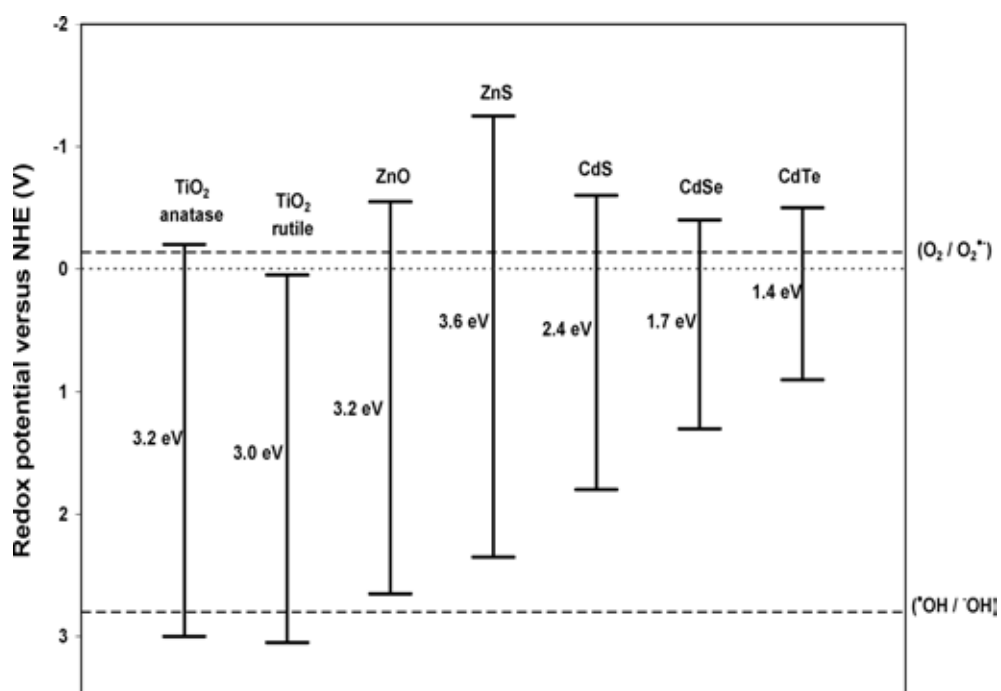
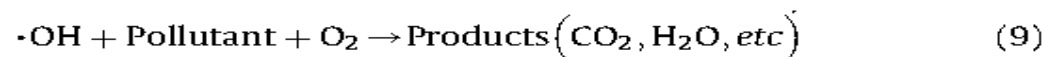
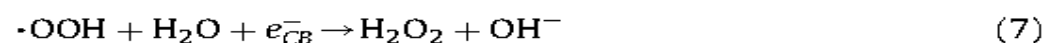


Figure 2.5 Band gaps, valence bands and conduction bands of semiconductors (Petlicki and van de Ven, 1998)

2.2.2 Reactions of TiO_2

Figure 2.6 shows the schematic diagram of the UV photocatalytic oxidation process of VOCs using TiO_2 as the catalyst. The ability of TiO_2 to degrade pollutants

photocatalytically is based on the strong oxidation and reduction potential of its valence band (VB) and conduction band (CB), respectively. Reaction begins when TiO₂ absorbs a photon when irradiated with UV light ranging from 300-400 nm. If the energy absorbed is equal or larger than the band gap, an electron moves from the VB to CB, generating an electron hole pair (h⁺ and e⁻). These highly active electron hole pairs can either recombine producing heat or be used to reduce or oxidize species at the semiconductor surface. The positive holes (h⁺) reacts with water to form the hydroxyl radical (OH•) while electrons react with molecular oxygen to form the superoxide anion (O₂⁻) which further reacts with H⁺ to produce the hydroxyl radical (OH•). Finally, the hydroxyl radical (OH•) generated reacts with pollutants to produce final end products (CO₂, H₂O and intermediate compounds). Equations (1) - (9) describe the reaction pathways using titanium dioxide (TiO₂) as a semiconductor.



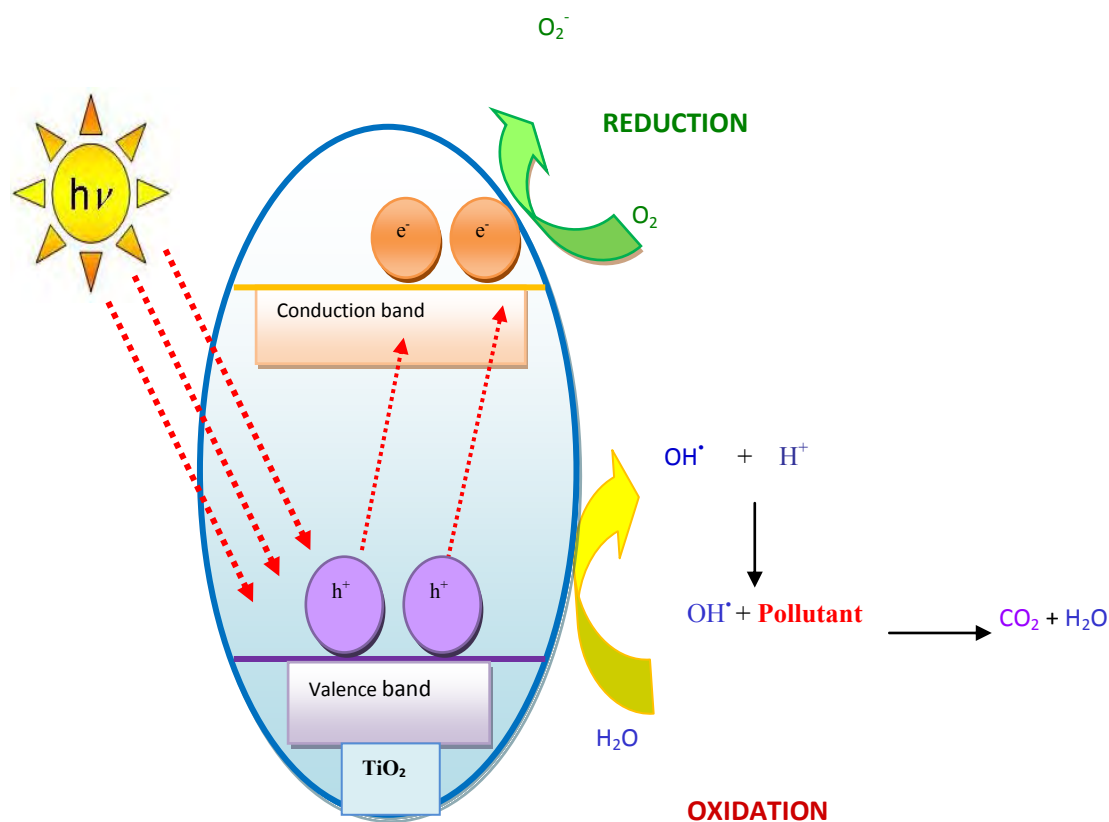


Figure 2.6 Photocatalysis and reaction mechanisms of TiO_2

(Yasushiro and Takayuki, 2008)

2.2.3 TiO_2 -based building materials

TiO_2 -based building materials have been used as coating materials on structures and walls for air purification (Poon and Cheung, 2007), self-disinfecting surfaces (Jun et al., 2001), self-cleaning surfaces (Shang et al., 2007) and for anti-fogging purposes (Wang et al., 2006). TiO_2 -based building materials are widely used in road structures such as pavement, road-blocks, soundproof walls, tunnel and paints wall and in building materials and interior furnishings such as paints, tiles wall paper, and window blinds.

Recent developments in the field of photocatalytic oxidation have led to a renewed interest in construction materials containing photocatalysts within the

framework of a strategy to eliminate air pollution. A current application of TiO₂-based materials under research is the use of TiO₂-based concrete for road pavements. One reason for the use of TiO₂-based concrete pavements is that optimal reactions of the pollutants may occur due to the close proximity of the motor vehicle emissions and the concrete pavements. Lackhoff et al. (2003) noted that cement is an important and popular substrate because of its relative low cost and large-scale application. Concrete structures with their large surfaces serve as a medium where air pollutants are sorbed and/or trapped which help to reduce pollutants in the atmosphere but at the same time make the concrete surfaces aesthetically dirty or unacceptable (Lackhoff et al., 2003; Cassar, 2004). Cassar (2004) showed that cement itself exhibits limited amounts of photocatalytic degradation but its photocatalytic reactions increased when TiO₂ was added. Cassar (2004) observed that the TiO₂-concrete mixture had photocatalytic effect that was higher than TiO₂ alone.

2.2.4 Parameters impacting photocatalytic efficiency

There are many environmental factors that affect the photocatalytic oxidation of TiO₂-based concrete material. Understanding these relationships will assist in predicting and obtaining a desired outcome and to develop the technology further for real world applications. Environmental factors impacting photocatalysis include pollutant types, pollution concentrations, relative humidity, air flow rate, UV light intensity, and the cleanliness of the surface of TiO₂-based material. However, in many situations; more than one environmental parameter may impact the photocatalytic effect, making it difficult to clearly identify the dominant environmental parameter.

Pollutants concentration

Providing the pervious study about the photocatalytic oxidation for various compounds which use the pollutants concentration as a parameter to study the PCO reactions. For example, Einaga et al. (1999) reported that the percent removal decreased from 90% to 10% when the benzene concentration increased from 80 to 260 ppmv. Ku et al. (2001) presented results that showed a change in percent removal from 80% to 55% when the trichloroethylene concentration of TCE increased

from 240 to 640 ppmv. The decrease in percent removal was attributed to the increase in mass transfer rate and the accumulation of oxidation products on the surface which in turn inhibit the absorption of pollutants and potentially lead to the deactivation of the photocatalysts (Ao et al. 2002; Demeestere et al., 2008). Other studies that showed similar results on the influence of pollutants concentration are Liu et al. (1997), Hager et al. (2000), Ku et al. (2001), Shen and Ku (2002) and Demeestere et al. (2004)

Relative humidity (RH)

Several researchers found that increasing the relative humidity would increase the degradation rates (Einaga et al., 1999, 2001; Belver et al., 2003; Jeong et al., 2005). For example, Einaga et al. (2002) reported that increasing relative humidity of benzene, toluene and cyclohexene was increased the pollutants reaction rates. Several studies indicated that the presence of water vapour may have an inhibiting effect or an activating effect or no effect on the photocatalytic oxidation reactions of VOCs (Guo et al., 2008, Takeuchi et al., 2010). An explanation for the inhibition was that water molecules compete with the pollutant molecules for available surfaces (Wang et al., 2007; Demeestere et al., 2008; Sleiman et al., 2009). Sleiman et al. (2009) demonstrated that water forms one or more layers of water film on the surface which may prevent the pollutant from reaching the TiO₂ layer. Einaga et al. (1999) reported that the percent removal of benzene in the gas-phase at 80 ppmv, increased from 5 to 92 % with an increase in relative humidity from 0 to 65 %. Many researchers found in their experiments that a higher relative humidity was supported by an increase in the formation of CO₂ (Blount and Falconer, 2002).

To successfully understand this technology, optimal humidity conditions for photocatalytic reactions should be identified. Liu et al. (2008) suggested a 55% relative humidity for the optimal removal of formaldehyde while Quici et al. (2010) proposed that at very low concentration of toluene a 10% RH was suitable for the optimal degradation in the presence of light and TiO₂. However, there seemed to be a discrepancy in whether an optimal relative humidity exists (Liu et al., 2008; Sleiman et al., 2009). For example, Sleiman et al. (2009) research on toluene photocatalytic oxidation showed that there was no optimum relative humidity and Ao et al. (2004)

were unable to find an optimal humidity level for degradation of formaldehyde. Ao et al. (2002) noted that the effect of water vapor (relative humidity) may be dependent on the pollutant type and its concentrations.

Light Intensity (I)

Many scientists have argued that photodegradation cannot occur in the absence of light (Zhao and Yang, 2003; Poon and Cheung, 2007; Liu et al., 2008). Consequently, a photocatalyst such as TiO₂ would need light as an energy source to degrade any pollutants. As described earlier in the photocatalytic reaction mechanism, the wavelength and quantity of photons (intensity) are basically responsible for the photocatalytic activity. A wavelength between 300-400 nm is required for the photoactivation of TiO₂. This wavelength range corresponds to the ultraviolet range. It has conclusively been shown that higher intensities of UV light (more photons) will result in higher photocatalytic oxidation rates (Zhao and Yang 2003).

Work done by Zhao and Yang (2003) showed that increasing the light intensity from 0.08 to 0.45 mW/cm² resulted in an increase in the degradation rate of TCE from 0.08 x 10⁻⁶ to 0.25x 10⁻⁶ mol/s g. Similarly, Strini et al. (2005) showed that enhancing the irradiance from 0 to 1500 μW/cm² resulted in an increase in the oxidation of o-xylene and ethylbenzene and a slight increase in the oxidation of benzene and toluene. The relationship between intensity and photocatalytic oxidation rates is generally linear (demeestere et al., 2012) while the oxidation rate is dependent upon the type of chemical pollutant. The intermediates formed are also dependent on the intensity. For example, Zhao and Yang (2003) demonstrated by using the germicidal lamps at a higher intensity, in higher oxidation rates and formation of more intermediates were obtained as compared to lower intensities using black lamps.

Flow rate (Q)

As previously noted, an increase in air flow rate has a negative impact on NO_x reduction efficiencies (Dylla et al., 2011). The faster flow rate means less contact time for the photocatalytic reaction to occur, resulting in lower reduction efficiencies. Demeestere et al. (2008) showed that higher removal efficiencies and lower concentrations of toluene were obtained when toluene was exposed for longer periods

to a TiO₂-based roof tiles. Similarly, Sleiman et al. (2009) showed an increase in flow rate resulted in a decrease in the removal efficiency of toluene from 95% to 65%. This is due to an increase in flow rate which tends to decrease the residence time in the photocatalytic reactor, and an increase in concentration of pollutants which tends to increase the mass transfer rate and accumulation of final products (Ao et al., 2002; Zhao and Yang, 2003).

Temperature

Compared to other environmental parameters, temperature is the less investigated as many of the experiments were performed at ambient temperature. Several studies reported benzene was showed no significant degradation effect of temperature ranging between 15 and 70°C but the generation of CO₂ was found to increase slightly (Hager and Bauer, 1999; Belver et al., 2003). In another study, Hager and Bauer (1999) reported maximum toluene degradation at 25 °C from the temperatures ranging between 5 and 75°C and they also recommend that the low number of adsorbed water molecules at high temperatures probably affected the generation of hydroxyl radicals which may be the cause for the decline in photocatalytic activity. In agreement with these results, Belver et al. (2003) demonstrated that toluene conversion decreased slightly with an increase in temperature from 70 to 140°C.

2.2.5 Data gaps and research questions about TiO₂ photocatalytic Oxidation

Although there are many evidence on the pollutant removal of photocatalytic building and construction materials, there are several observations and problems when these materials are used in full-scale applications. Since the TiO₂ is immobilized in the construction material, there may be significant loss in photocatalytic activity since a majority of the TiO₂ is embedded in the concrete. Rachel et al. (2002) maintained that TiO₂ slurries in decomposing 3-nitrobenzenesulfonic in water were showed more efficient than TiO₂-cement modifies and TiO₂ - red bricks, moreover; Rachel et al. (2002) meditated that the catalytic activity loss probably comes from the presence of

ionic species which would be reduction of active surface. However, mechanisms leading to catalyst deactivation are not fully clear therefore a better understanding and knowledge of catalyst lifetime and of parameters affecting catalyst deactivation is of major importance for the applicability of heterogeneous photocatalytic technology.

A second issue is the production of intermediates and by products and the accumulation of inert materials such as clays and soot with time on the surface which will decrease the photoactivity by blocking reactive sites (Ameen and Raupp, 1999; Martra et al., 1999; Cao et al., 2000; Blount and Falconer, 2002; Einaga et al., 2002). In addition, generation of undesirable intermediates with worst environmental and health impact than the starting pollutants may strongly affect the application of photocatalyst-based materials.

Another issue that needs further investigation is the impact of aging of the TiO₂-based materials. Lackhoff et al. (2003) stated that the carbonation of the TiO₂-modified cements with time (over several months) led to changes in cement surface structure and a noticeable loss in catalytic efficiency. A report published by the Hong Kong Environmental Protection Department claimed that the photocatalytic activity of TiO₂-coated paving blocks decreased significantly after 4 months of exposure in a downtown area due to the accumulation of contaminants on the block surface (Yu, 2003).

A serious weakness in the literature available is that research work are not standardized, i.e., many articles cannot be compared to each other, due to differences in environmental parameters such as light, amount of catalyst, reactor set-up, reaction time, and type and concentration of pollutants used. Another question that needs to be addressed is the fate and transport of the photocatalytic materials used which are usually added as nano-materials and the possible health effects of nano-materials and the byproducts formed in incomplete photo-oxidation (Yu, 2003). The particle size of nanoscopic photocatalysts is so small that it is possible for the materials to enter the human body triggering adverse health effects (Wang et al., 2008).

2.3 Air Purification of Nitrogen Oxide (NO_x)

2.3.1 Background, qualification and toxicity

NO_x is a group of highly reactive gases consisting of nitric oxide (NO) and nitrogen dioxide (NO₂). These compounds originate from combustion of fuels at high temperatures (EPA, 2010). NO_x is one of the six major pollutants listed as a criteria pollutant in the ambient air quality standards required by the Clean Air Act 1970 (Tao et al., 2010). A negative effect associated with NO_x emissions is the formation of troposphere ozone when NO_x reacts with volatile organic compounds in the presence of sunlight. Ozone can cause adverse effects such as damage to lung tissue and reduction in lung function in susceptible populations. The American Lung Association estimates that nearly 50 % of United States inhabitants live in areas that are not ozone compliance (EPA, 2010).

Numerous studies have shown that short term exposures to high concentrations of NO_x can have negative effects on human health (McConnel et al., 2010). Mobile sources contribute up to 58% of NO_x pollution emitted in the United States (EPA, 2010). The concentration of NO_x increases in areas with high traffic density (Jimenez et al., 1999). Compared to ambient concentrations, NO_x concentrations for in-vehicle microenvironment and near-roadway microenvironment are 200 –300% higher and 30–100% higher, respectively (EPA, 2011).

2.3.2 Current work to eliminate nitrogen oxide (NO_x)

Recently, several studies have been presented to illustrate the use of self-cleaning concrete for air remediation purposes to degrade nitrogen oxides (NO_x) and volatile organic compounds (VOCs). Due to the increase in use of photocatalytic materials for air purification, a Japanese standard was issued for the evaluation of the air purification materials for the removal of nitric oxide in 2004 (JIS R 1701-1, 2004). A few years later, the International Organization for Standardization (ISO) published its own version of a test to evaluate the performance of photocatalytic materials (ISO 22197-1, 2007). Some earlier studies include work done by Murata et al. (1999) on TiO₂ concrete blocks air purifying pavement for NO_x degradation and

work by Cassar (2004) on the combined use of TiO₂ and cement for the synergistic effects of photocatalytic reduction of NO_x.

Since the publication of the Japanese and ISO standard test, experiments have been conducted to answer several of the issues facing the use of TiO₂-based materials for air pollution mitigation. Poon and Cheung (2007) evaluated paving blocks made by waste materials and TiO₂ for NO removal and found that an optimum mix design consisting of recycled glass, sand, cement and 10% TiO₂ removed maximum at 4 mg/hr/m² of NO removal. Husken et al. (2007) carried out a comparative analysis of different photocatalytic cementitious products under laboratory conditions and found that NO_x degradation varied significantly, with some cementitious products achieving 40% degradation whereas others showed almost no effect. Poon et al. (2007) and Chen et al. (2008) observed that incorporating recycled glass cullets in cementitious paving blocks gave rise to enhanced photocatalytic activity towards NO degradation. This enhanced effect can be explained by the increased porosity and light transmittance effects. The same authors also reported that long curing ages may lead to a significant loss of photocatalytic activity - probably due to a change in the internal microstructure of concrete caused by cement hydration (Chen et al., 2008). Similarly, Husken et al. (2009) recently found that the extent of substrate roughness of the photocatalytic concrete helped in NO_x degradation.

Recent research has shown that a thin surface coating of TiO₂ is able to remove a significant portion of NO from the atmosphere when placed as close as possible to the source of pollution (Dylla et al., 2010). Likewise, Hassan et al. (2010) evaluated three application methods of TiO₂ onto concrete pavement. These methods were an ultrathin cementitious-based coating, a water-based TiO₂ solution and a sprinkling of TiO₂ to the fresh concrete surface before hardening. TiO₂ incorporated into an ultrathin cementitious surface layer was more durable than the other two methods while maintaining high environmental removal efficiencies. These studies, however, did not fully address the effectiveness of the photocatalytic compounds, and the reaction mechanisms and rates. The fate of reaction products such as whether all the NO_x was oxidized by photocatalytic concrete, whether the end products precipitate on the concrete, and the effect of NO₂ and NO mixtures on degradation

rates have not been evaluated. If nitrate salts were produced, will they be removed from concrete surface by rain and significantly pollute surface water.

Some studies have reported lower photocatalytic activity of TiO_2 when used in immobilized form rather than in suspended form (Rachel et al., 2002) due to lower availability of TiO_2 reactive surfaces and possible inhibition of other compounds. Lackhoff et al. (2003) reported a decreased in atrazine degradation and attributed the decrease to cement carbonation over time.

TiO_2 -modified cement is already commercially available (Cassar and Pepe, 1998) and has been successfully used in several European constructions and monuments, such as the Roman Catholic Church “Dives in Misericordia” in Rome, Italy and the “Cité des Arts et de la Musique” palace in Chambéry, France. The utilization of TiO_2 -modified cement was studied in Europe under the Photocatalytic Innovative Covering Applications for Depollution Assessment (PICADA) program. Several projects were carried out to verify the effectiveness of the photocatalytic cementitious materials under ambient conditions. For example, a street in the city centre of Bergamo, Italy was re-paved with photocatalytic concrete paving blocks to a total surface area of about 12,000 m^2 . Monitoring equipment placed at two locations (one at the area where photocatalytic blocks were laid and the other at the extension of the road paved by normal bituminous concrete as a reference) showed an average NO_x abatement of 45% during the day from 9 am to 5 pm (Guerrini et al., 2007). A similar project was carried out in Antwerp, Belgium, where 10,000 m^2 of photocatalytic pavement blocks were laid on a parking lane. Measurements at the site indicated a decrease in NO_x peak concentrations due to the presence of the photocatalytic materials. The photocatalytic activities of these blocks was retested in the laboratory after they were in service for two years and were found to show no reduction in NO_x removal efficiency after the paving blocks were washed with distilled water (Beeldens, 2007). In Guerville, France, three artificial street canyons were built to evaluate the depollution performance of walls covered with photocatalytic concrete. Continuous monitoring of NO_x concentrations in the TiO_2 -treated street canyon showed NO_x concentrations that were 36.7–82.0% lower than the concentrations observed in the reference canyons (Maggos et al., 2008).

In summary, the self-cleaning and depollution properties of TiO₂-based cementitious materials have been evaluated in laboratory-scale (Strini et al., 2005; Poon and Cheung, 2007; Demeestere et al., 2008; Ruot et al., 2009) and at full-scale applications (Cassar et al., 2007; Maggos et al., 2008) with the main focus on the decontamination of NO_x (Poon and Cheung, 2007; Husken et al., 2009; Ballari et al., 2011). Table 2-2 provides a summary of NO_x change in the presence of various environmental parameters. There are several studies that investigated the removal of volatile organic compounds (VOCs), such as BTEX (Strini et al., 2005; Demeestere et al., 2008; Ramirez et al., 2010). However, only a few studies paid attention to the direct impact of the cementitious materials on the final photocatalytic performances (Chen and Poon, 2009) and the characteristics of the TiO₂ on the surface that are responsible for the photocatalytic reaction (Ruot et al., 2009)



























2.4 Air purification of Volatile Organic Compounds (VOCs)

2.4.1. Background, qualification and toxicity

VOCs are classified by the World Health Organization (WHO) as all organic compounds excluding pesticides with boiling points in the range of 50 to 260°C. VOCs are typically higher in indoor environments than in outdoor environments. However, outdoor air is considered a source for indoor VOC pollution. Although the largest source of VOCs pollution is from building materials, motor vehicles are responsible for about 29% (Kuhns et al., 2004). For example, aromatic hydrocarbons such as toluene, xylenes, ethylbenzene, trimethylbenzenes, and aliphatic hydrocarbons are found in gasoline and in incomplete combustion of gasoline (Wang et al., 2007). These petroleum hydrocarbons are the most common VOCs found in both indoor and outdoor environments (Ao et al., 2004).

Among the many VOCs emitted from mobile sources, benzene, toluene, ethylbenzene and xylenes (BTEX) are of major concern and are in the list of 189 hazardous air pollutants in the 1990 Clean Air Act. Benzene is a human carcinogen (Category A) whereas ethylbenzene has been classified by the International Agency for Research on Cancer (IARC) as a Group 2B carcinogen. Not much is known about

Table 2.2 Impact of environmental parameters on the rate of NO_x degradation (adapted from Joel Sikkema, 2012)

Parameter	Change	Change in NO _x Degradation Rate	References
Irradiance			Husken et al., 2009; Ballari et al., 2011; Beeldens et al., 2011
Relative humidity (RH)			Husken et al., 2009; Dylla et al., 2010; Ballari et al., 2011; Dylla et al., 2011
NO _x concentration			Husken et al., 2009; Ballari et al., 2010; Ballari et al., 2011; Beeldens et al., 2011
NO _x /NO ₂ ratio			Dylla et al., 2011
Flow rate through reactor			Husken et al., 2009; Ballari et al., 2010; Dylla et al., 2010; Dylla et al., 2011
Air way path height			Ballari et al., 2010
TiO ₂ concentration			Husken et al., 2009; Dylla et al., 2010
TiO ₂ specific surface area			Husken et al., 2009
Pavement specific surface area			Husken et al., 2009; Dylla et al., 2010; Dylla et al., 2011
Homogeneity of TiO ₂ distribution			Husken et al., 2009
Color pigment			Husken et al., 2009
Pavement age			Beeldens et al., 2011
Roadway contaminants			Dylla et al., 2011

? - Inconclusive



















The reaction of BTEX with TiO₂-based concrete pavements. Currently, a standard test for testing VOCs has not been developed yet (Anibal et al., 2010).


2.4.2. Current work to eliminate VOCs

Several researchers reported that the reaction efficiency of BTEX was dependent on the amount of BTEX adsorbed on the TiO₂ catalyst (Hennezel and Ollis, 1997; Ao et al., 2002). Strini et al., (2005) examined the degradation of BTEX mixture gas by using TiO₂ powder mixed with white Portland cement and found that the percent removal ranged between 5% and 54% and o-xylene was showed the highest photocatalytic activity, followed by ethylbenzene, toluene and benzene. Strini and co-workers observed that the degradation rate of BTEX of pure TiO₂ was 3-10 times greater than a cementitious sample with 3% TiO₂ and the degradation rates were dependent on the concentrations of the BTEX and the intensity. However, the photocatalytic activity was not dependent on the TiO₂ content. Demeestere et al. (2008) studied toluene degradation by using TiO₂ as a photocatalyst in building materials. Their experiments were focused on the effect of pollutant concentration, air relative humidity and gas flow rate. They found that at high inlet concentration and relative humidity was presented low toluene removal efficiency, whereas better performance was noticed with increased residence time in the reactor. Under the proper conditions percent removal were reached up $78 \pm 2\%$. Anibal et al. (2010) studied eight cementitious materials enriched with TiO₂ by using two different coating methods which were dip-coating and sol-gel and found that high percent removal (up to 86%) were obtained with the dip-coated samples. Figure 2.3 presents the probable change in the degradation rate of BTEX for a change in the environmental parameter.

Since there are not many studies on the reaction of VOCs with the TiO₂-based cementitious materials, there are many questions regarding the reaction rates of various VOCs, the reaction mechanisms, the fate of reaction products especially potentially hazardous chemicals, and the effect of environmental parameters. Outdoor testings of these cementitious materials are limited where conditions such as blinding due to inert materials may affect the degradation efficiency of these materials.

Table 2.3 Impact of environmental parameters on the degradation rate of BTEX

Parameter	Change	Change in BTEX Degradation Rate	References
VOCs concentration			Einaga et al.,1999; Ku et al., 2001; Ao et al., 2002; Demeestere et al., 2008; Sleiman et al., 2009
Relative humidity (RH)			Hager and Bauer,1999; Einaga et al., 1999, 2001, 2002; Maira et al., 2001b; Kim and Hong, 2002; Belver et al., 2003; Jeong et al., 2005
Light Intensity (I)			Fujishima et al., 2000; Zhao and Yang, 2003; Strini et al.,2005
Flow rate (Q) (↑ velocity and ↓ residence time)			Ao et al., 2002; Zhao and Yang 2003; Demeestere et al.,2008; Sleiman et al., 2009
Temperature			Hager and Bauer ,1999; Belver et al., 2003
Ageing of slab			Lackhoff et al., 2003; Yu, 2012
Regeneration of intermediates			Ameen and Raupp, 1999; Martra et al.,1999; Cao et al., 2000; Blount and Falconer, 2002; Einaga et al., 2002
Oxygen concentration			Demeestere et al.,2007
Roadway contaminants			-

 - Inconclusive or no data available

Development of a model to describe the mass transport and photocatalytic reaction of various pollutants under various realistic scenarios will be helpful in predicting the effectiveness of the cementitious materials for other conditions that were not tested in the laboratory. In addition, the effectiveness of TiO_2 in colored matrix should be evaluated if the materials are to be used widely as building materials.

CHAPTER III METHODOLOGY

3.1 Materials and Apparatus

3.1.1 Chemicals

- 10 ppmv of benzene, toluene, ethylbenzene and xylenes each provided by Praxair, Inc. (Danbury, CT, USA)
- Polymethyl methacrylate (PMMA)
- Cement (Type I) and cement (TiO₂-based) (Buzzi Unicem, Selma, MO, USA)
- Fine aggregate (ASTM C778 standard sand, U.S. Silica Co., Bridgeton, MO, USA)
- Nanopure water

3.1.2 Instruments and laboratory-ware

- Black Light Blue (BLB) fluorescent lamps 15 W UV-A illumination (15BLB, Ultra-Violet Products, LLC, Tokyo, Japan)
- UV radiometer (VLX-3W, Vilber Lourmet, Eberhardzell, Germany)
- Mass flow controller (GFC MFC, Aalborg, Orangeburg, NY, USA)
- Traceable hygrometer (Cole-Parmer, Vernon Hills, IL, USA)
- Gastight sample lock syringe (Hamilton, Reno, NV, USA)
- Gas Chromatography with Photo Ionization Detector (Tracor 540 GC/PID, Madrid, Spain)
- Headspace vials aluminum seal with septa and crimp (Restek, Bellefonte, PA, USA)
- Oven
- Gas washing bottle
- Miscellaneous laboratory glassware



Figure 3.1 Traceable hygrometer and UV radiometer



Figure 3.2 Mass flow controller and Black Light Blue (BLB) fluorescent lamps
15 W UV-A illumination



Figure 3.3 Headspace vials and aluminum seal with septa and Crimp

3.2 Experimental Procedures

3.2.1 Preparation of photocatalytic concrete slabs

Preparation of concrete slabs was based on the concrete mix design of the Missouri Department of Transportation (MoDOT). Components of the concrete mix were cement (cement with TiO_2 or Type I cement), fine aggregate (ASTM C778 standard sand, U.S. Silica Co.) and water which were mixed in the following proportions: 624 kg/m^3 , 262 kg/m^3 and 1412 kg/m^3 respectively. Given the small volume of the slabs prepared, the mix did not include coarse aggregate (Sikkema et al., 2012). Concrete slabs prepared measured $152 \text{ mm} \times 152 \text{ mm} \times 25 \text{ mm}$ ($23,104 \text{ mm}^2$ exposed area). The slabs were made by using a two-lift procedure with equal volumes of a Type I cement for the bottom lift followed by the photocatalytic-active cement for the top lift. TiO_2 was mixed into the cement rather than a surface coating as abrasion from the tires of the motor vehicles would rapidly remove the TiO_2 from the surface of the cement.

Immediately after pouring the first and second lift, a damp cloth and plastic sheet were laid over the slab surface for a 24-h period while the slab cured. The slabs were then removed from their forms and cured for 14 days in 100% relative humidity. The concrete slab was then cleaned by immersing in nanopure water for 2 hours and then dried for 20 hours in an oven at 60°C . The concrete slab was then wrapped in aluminum foil and sealed in a plastic bag until use. The procedure used in the

preparation of the slab was similar to that employed by the International Organization for Standardization (ISO) Standard 22197-1:2007(E). Figure 3.1 shows a typical concrete slab used for testing while Figure 3.2 shows the procedure to make the concrete slab.



Figure 3.4 Typical concrete slab for laboratory- scale testing

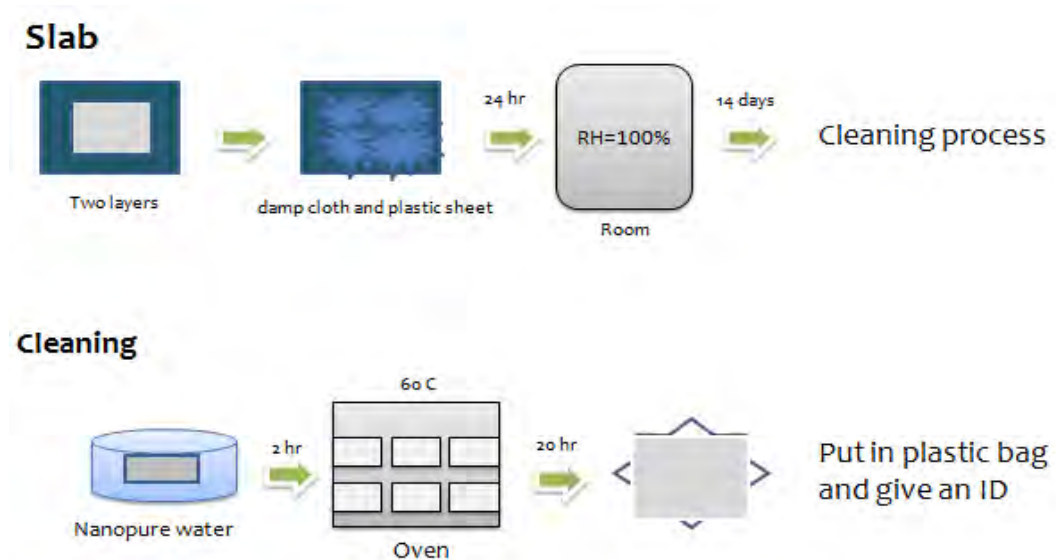


Figure 3.5 Method for making TiO_2 -based concrete slabs

3.2.2 Laboratory setup

Experiments were conducted in a laboratory-scale photoreactor which was built and adapted according to ISO 22197-1: Test Method for Air Purification Performance of Semiconducting Photocatalytic Materials - Part 1: Removal of Nitric Oxide (Sikkema et al., 2012). The schematic diagram of the experiment apparatus is shown in Figure 3.3. The photoreactor was made of polymethyl methacrylate material (PMMA) and its dimensions were 1.9 m long, 0.45 m wide and 0.68 m high. A TiO₂ slab was placed in the photoreactor with an air gap of 5 mm between the concrete slab and a borosilicate glass window. The photoreactor and its associated pipings were checked for air tightness before each test. The experimental setup was operated in a continuous flow-through mode using house air and a tank containing 10 ppmv of each of the BTEX compounds in nitrogen gas (Praxair, Inc., Danbury, CT, USA). Both house air and BTEX gas flow rates were carefully controlled using mass flow controllers (GFC MFC, Aalborg, Orangeburg, NY, USA). Part or all of the house air was saturated with water using a gas washing bottle and then mixed with the BTEX gas to obtain various BTEX concentrations and relative humidity in the gas mixture. A traceable hygrometer (Cole-Parmer, Vernon Hills, IL, USA) was used to measure the relative humidity and temperature. The BTEX gas then flowed over through a cross section with a width of 150 mm consisting of the concrete slab. The space between the concrete slab and the borosilicate glass window was approximately 5mm. UV irradiation was provided by 15 W UV-A (black-light blue) fluorescent lamps (XX-15BLB, Ultra-Violet Products, LLC, Tokyo, Japan) at an irradiance intensity between 0.5 - 12 W/m². The UV irradiance was measured by an UV radiometer (VLX-3W, Vilber Lourmet, Eberhardzell, Germany). A gas sampling point was located after the photoreactor. By using the by-pass mode (no air flow into the photoreactor), the inlet concentrations of five target pollutants (benzene, toluene, ethylbenzene and o-, m-, p-xylenes) were measured. After determining the inlet concentration, the by-pass mode was switched over to the photoreactor mode where the air flowed over the concrete slab. The photoreactor was operated in this mode for at least 10 minutes to reach steady state conditions before an air sample was collected from the sampling port to determine the amount of target pollutants removed.

Environment parameters studied include BTEX concentrations, relative humidity (RH), flow rate (Q), UV intensity (I), ageing of the slab and partially covering the slab by dirt taken from a full-scale site). The environmental parameters and their conditions used in the experiments are shown in Table 3.1. The experimental matrix is presented in Table 3.2.

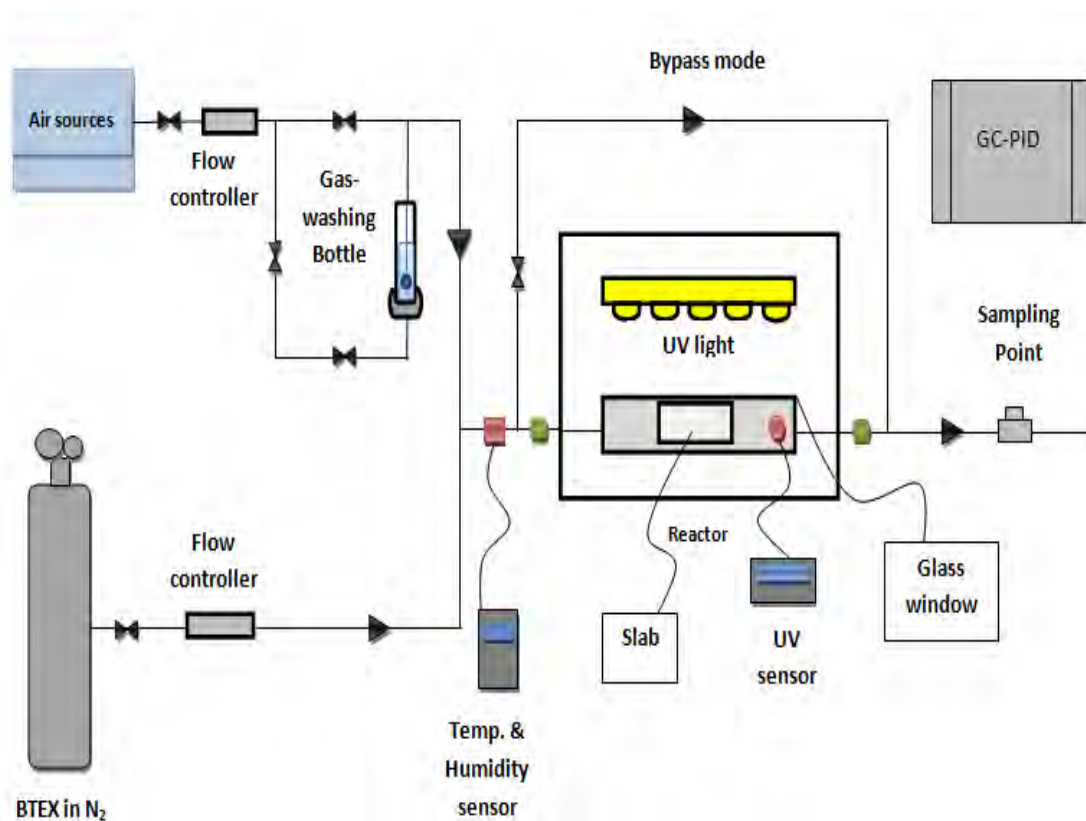


Figure 3.6 Schematic diagrams of experimental apparatus
(adapted from Ballari et al., 2011)



Figure 3.7 Experiment setup in the laboratory at the Department of Civil, Construction and Environmental Engineering, Iowa State University, USA



Figure 3.8 10 ppmv BTEX gas mixture for the experiment

Table 3.1 Environmental parameters used in the study

Parameter	Approximate Values Used
Relative Humidity (%)	10, 25, 50, 70
Flow rate (L/min) (Air velocity m/s)	1, 3, 5 (0.02, 0.07, 0.11)
Intensity (w/m^2)	5, 10, 12
VOC concentrations Benzene, toluene, ethylbenzene and mixed isomers (o-,m-,p-Xylenes)	1 ppmv for each VOC
UV light source	Blacklight blue fluorescent lamps

Table 3.2 Experimental matrix for lab-scale photoreactor tests

Change in Parameter	Expt. Run	BTEX Conc. (ppmv)	Relative Humidity (%)	Intensity (W/m^2)	Flow Rate (L/min)	Pavement age (months)
Relative Humidity	1	1	10	10	3	0
	2	1	25	10	3	0
	3	1	50	10	3	0
	4	1	70	10	3	0
UV Intensity	5	1	50	5	3	0
	6	1	50	12	3	0
Air flow rate	7	1	50	10	1	0
	8	1	50	10	5	0
Aging	9	1	50	10	3	1
	10	1	50	10	3	3

3.2.3 Analytical method

One mL of air sample was collected from the sampling port using a 1 mL gastight lock syringe (Hamilton, Reno, NV, USA) with a removable needle. The sample was directly injected into a Tracor 540 Gas Chromatograph with photo ionization detector (GC/PID) (see Figure 3.4). The GC was equipped with a 2 m column with an internal diameter 2 mm and packed with 1% SP1000 on Carbopack B 60/80 mesh. Helium was used as a carrier gas with a flow rate of 40 mL/min. The initial GC oven temperature was set at 50 °C for 3 min, ramped to 220 °C at 8 °C/min, and held at this temperature to elute late peaks while the injection and detector port temperatures were kept constant at 175 °C and 250 °C, respectively. Peak areas were integrated using the EZ Chrom Elite Software. To evaluate the performance of TiO₂-based concrete on BTEX degradation, the mass removed per unit time per unit area of the slab were estimated.



Figure 3.9 One mL syringe and Tracor 540 gas chromatograph

3.2.4 Operational procedure

The procedures for the operation of the photoreactor were as follows:

1. A concrete slab was placed in the reactor cell.
2. The quartz panel was cleaned with Windex and Kimwipes and was carefully laid on the photoreactor over the slab by minimizing any finger prints.

3. The quartz panel was then sealed to the photoreactor using plumber's putty.
4. All valves and all connections to the mass flow controller and gas washing bottle were checked and set to bypass mode.
5. The house air was turned on.
6. The BTEX gas tank was turned on.
7. The gases were adjusted using the mass flow controller to obtain the desired flow rate, concentration, and relative humidity.
8. The gas was allowed to pass for 10 min.
9. A 1 mL gas sample was taken from the sampling point and directly injected into GC-PID to measure the inlet concentration.
10. By closing and opening the required valves, the by-pass mode was switched to the photoreactor mode and the UV light source was turned on as showed in Fig. 3.7
11. The gas was allowed to pass though the photoreactor for 10 min
12. A 1 mL gas sample was taken from the sampling point and directly injected into the GC-PID to measure the outlet concentration after reacting with the slab.
13. The UV light was turned off and valves opened and closed to switch to the bypass mode.
14. The necessary valves, flow rates, humidity were then adjusted for the next experimental run.



Figure 3.10 Experiment with the UV light source on

CHAPTER IV

RESULT AND DISCUSSIONS

4.1 Photocatalytic Degradation of BTEX

Calibration curves for each compound for the gas chromatograph are presented in Appendix A. The concentrations obtained from the gas chromatograph were analyzed and reported as the mass of organic compound removed per unit time per unit surface area. The exposed area used was 23,104 mm². In addition, the percent removed were also estimated. The equations for estimating the mass removed per unit time per unit surface area and percent removal are presented in Appendix B.

Control experiments were conducted as follows: experiments with a concrete slab without TiO₂ in the bypass and reaction mode (with UV light off) and experiments with a concrete slab with TiO₂ with UV light on in the bypass and reaction mode. BTEX concentrations for the reaction mode were about the same as the BTEX concentrations in the bypass mode as shown in Fig.4.1. Based on these control experiments, it can be concluded that adsorption to the surface of the concrete slab was minimal and photocatalytic oxidation was minimal when the UV light was not on.

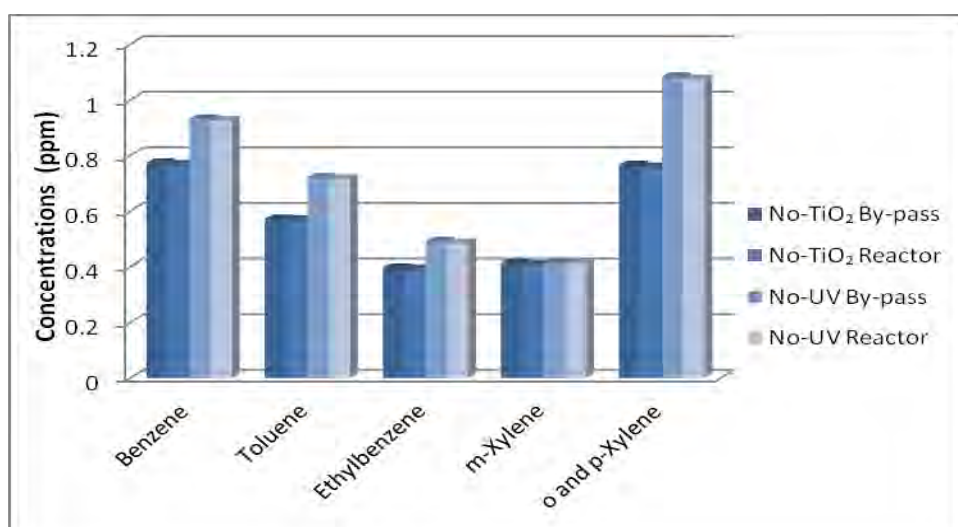


Figure 4.1 The Control experiment for non-TX active cement (no TiO₂) and non- UV light

4.2 Effect of relative humidity on BTEX Degradation

Fig. 4.2 shows the mass removal per time per unit area [$\text{mg}/(\text{hr}\cdot\text{m}^2)$] of each BTEX compound in the presence of UV light source for four different RHs (10%, 25%, 50% and 70%). The flow rate was kept constant at 3 L/min and the UV intensity was $10 \text{ W}/\text{m}^2$. The RH used covered the typical ambient air humidity range. For each RH, the inlet BTEX concentration was measured in the bypass mode and then the air was passed over the concrete slab and the outlet BTEX concentrations measured. As indicated in Fig. 4.2, the mass removal of toluene, ethylbenzene, m-xylene and o, p-xylene increased with an increase in RH from 10% to 50%. These findings of the current study are consistent with those previous studies such as Einaga et al. (1999 and 2002), Belver et al. (2003) and Jeong et al. (2005). For example, Einaga et al. (2002) indicated that an increase in the RH increased the reaction rate of benzene and toluene.

In this study, the mass removed per unit time per unit area was lower for a RH of 70% as compared to a RH of 50%. For benzene, the percent removed at 25% RH experiment showed a slightly lower mass removed than the mass removed at 10% RH. The difference may not be statistically significant. Other than that the trend for benzene removal was similar to that of the other BTEX compounds. It can be seen from the Fig.4.2 that the optimal RH for BTEX removal was at a RH of about 50%. If the RH is low (10%) or high ($> 70\%$) RH, water vapor on the surface of the slab has a negative effect on removal of BTEX. The presence of water on the surface produces hydroxyl radicals which in turn degrade the BTEX. However, low RH would mean a lower coverage of water molecules on the surface and therefore would not generate sufficient hydroxyl radicals while a higher RH would result in the surface covered with water which would require the BTEX to dissolve into the water layer before they can react with the hydroxyl radicals. This finding is in agreement with the findings of Sleiman et al. (2009) who showed that water forms one or more layers of water film which require the BTEX to dissolve into the water layer before they can react with the hydroxyl radicals. It is possible that the part of the mass removed could be due to adsorption rather than photocatalytic degradation.

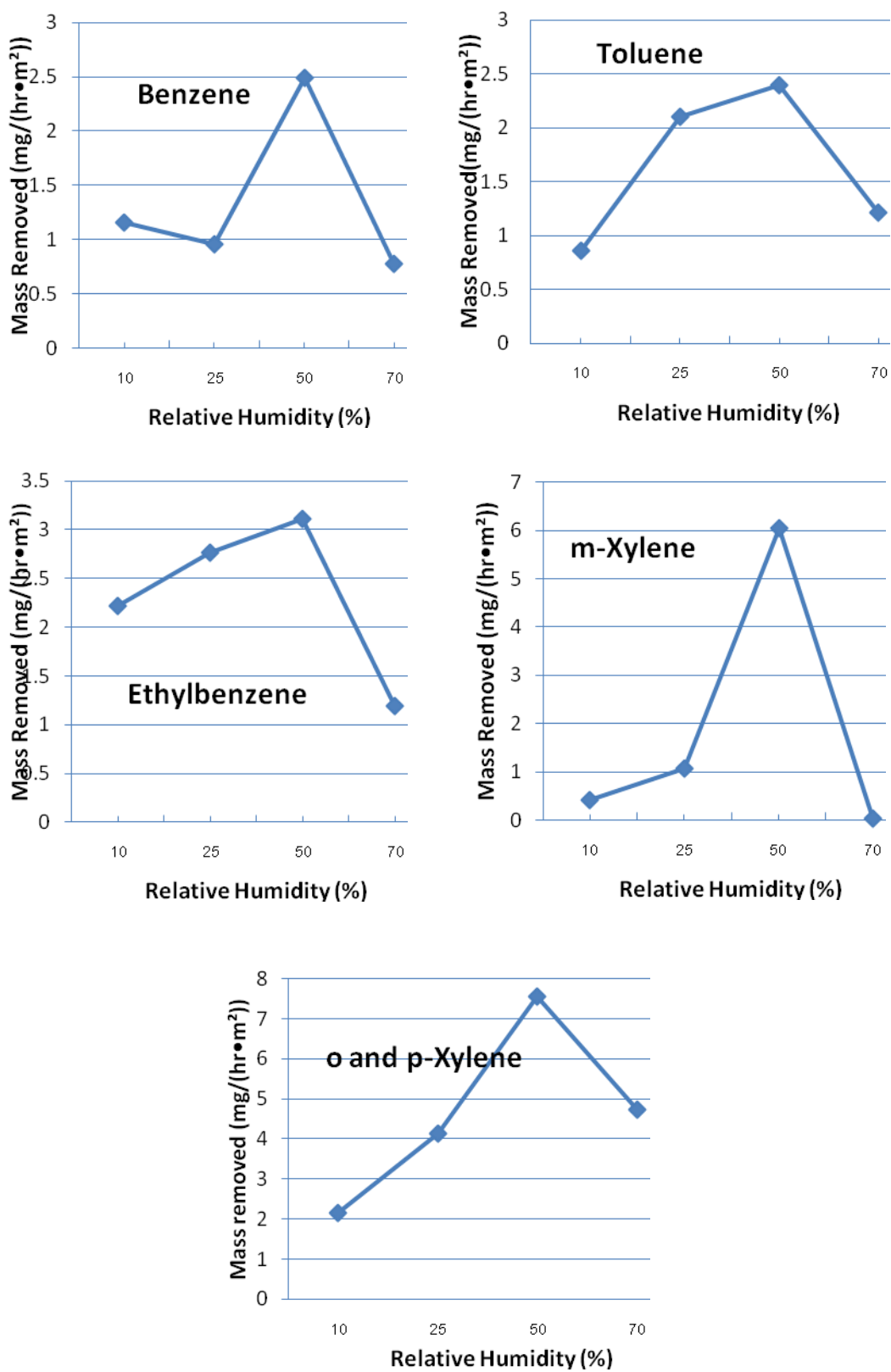


Figure 4.2 Mass of BTEX removed for different relative humidities

The experimental procedure used did not allow the removal mechanisms to be differentiated. However, the mass adsorbed may be assumed to be much lower than the mass degraded. Overall, the interest in this study is to assess the total mass removed by the TiO₂-based concrete slab.

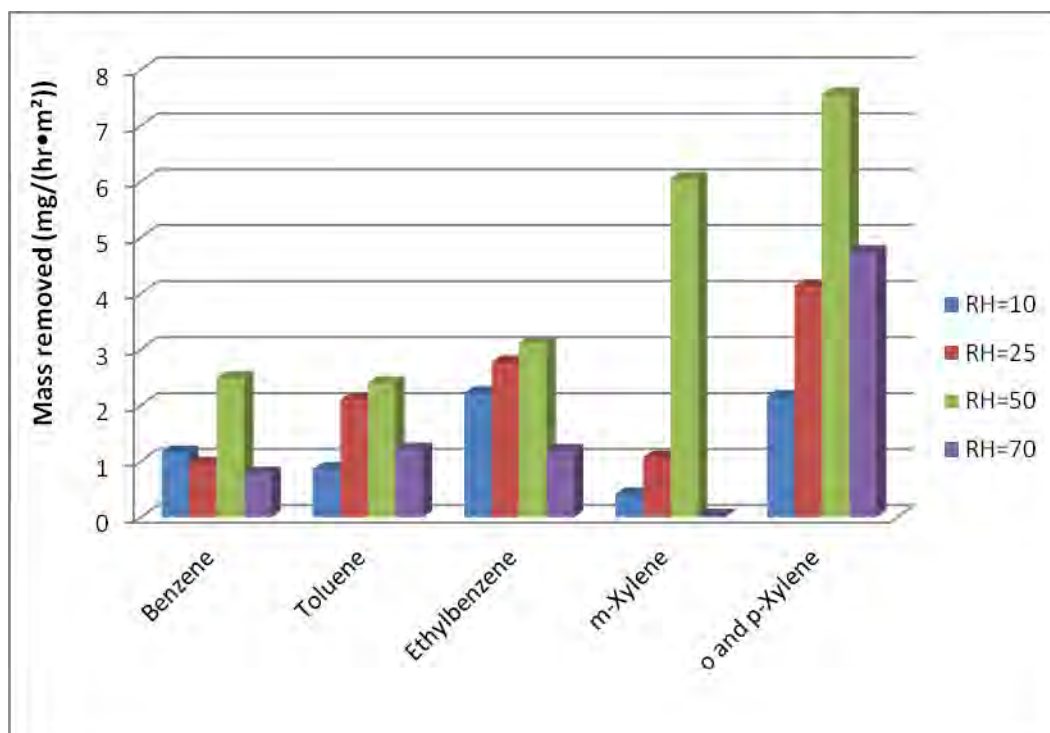


Figure 4.3 Bar chart of mass of BTEX removed for different relative humidities

Figure 4.3 presents the mass removed for each BTEX compound for all four relative humidities together on one graph. The results showed that o and p-xylene were more readily oxidized than the other BTEX compounds. The order from the most difficult to oxidize to the most readily oxidized compounds was benzene > toluene > ethylbenzene > o and p-xylene. This is in good agreement with the previous studies of Strini et al. (2005) and Christos et al. (2011). For m-xylene, the results showed that a 50% RH was the most suitable relative humidity with a significantly higher photocatalytic oxidation reaction as shown in Fig. 4.3.

It can be summarized from this set of experiment that a 50% RH was the optimum experimental conditions for the degradation of BTEX compounds in the air stream.

4.3 Effect of flow rate on BTEX degradation of BTEX

The effects of flow rate on benzene and toluene degradation are presented in Fig. 4.4. The flow rates in the experiments were 1, 3 and 5 L/min while the RH was set at 50% and the intensity was at 10 W/m². Based on the percent removal for benzene (Fig. 4.4 a and c), there was a trend of decreasing percent removal when the flow rate increased from 1 L/min to 5 L/min. This was probably true as the residence time for BTEX compounds would be the lowest for a flow rate of 5 L/min and therefore provided less contact time and reaction time. These findings are consistent with those of Sleiman et al. (2009) who found that an increase in flow rate decreased the removal efficiency of toluene from 95% to 65%. Similarly, Demeestere et al. (2008) reported that longer gas residence time for toluene exposed to TiO₂ roof tiles resulted in a lower amount of toluene and a correspondingly increase in removal efficiencies.

However, when the mass removed per unit time and per unit area was estimated (Fig. 4.4 b and d) the trend was opposite to that for percent removal with a gradual increase in mass removed when flow rate increased from 1 L/min to 5 L/min. This may be explained by the higher mass per unit time for a higher flow rate and therefore even though the percent removal decreased with higher flow rate, the total mass removed was higher due to the higher mass input per unit time into the photoreactor.

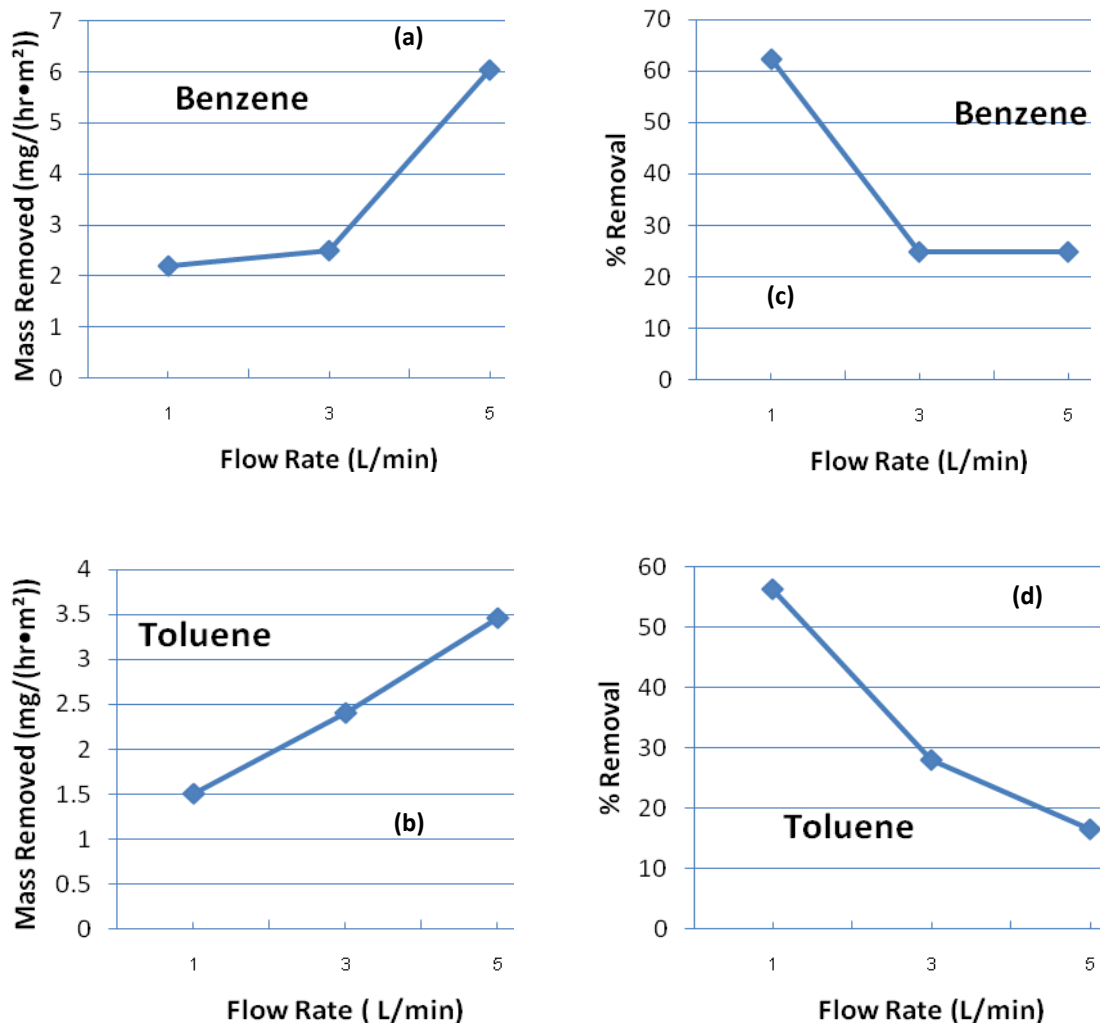


Figure 4.4 Percent removal and mass removed for benzene (a and c) and toluene (b and d) for different flow rates

Fig. 4.5 presents all the data on the effect of flow rate on BTEX degradation in one graph. The results showed that o and p-xylene were the most readily to oxidize. The order from the most difficult to oxidize to the most readily oxidized compounds was toluene > benzene > ethylbenzene > o and p-xylene.

It can be summarized from this set of experiment that the mass degraded was a function of the flow rate with of m-xylenes.

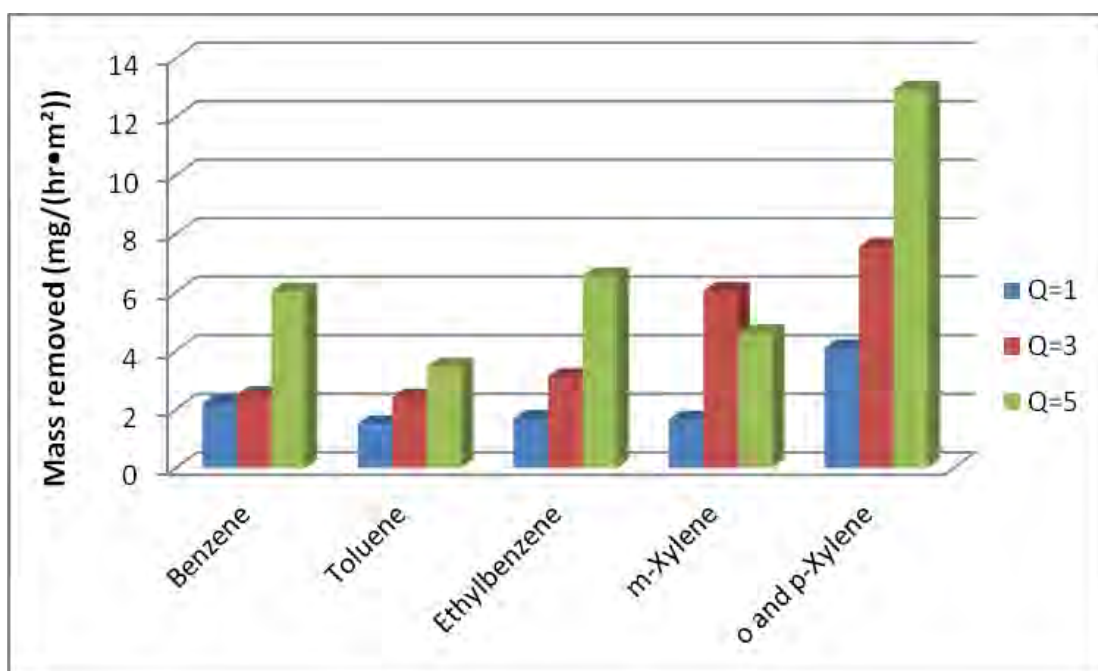


Figure 4.5 Mass removed of BTEX for different flow rate

4.4 Effect of UV intensity on BTEX degradation

The third set of analyses examined the impact of UV intensity. As shown in Fig. 4.6, the mass removals per time per unit area for each BTEX compound exposed to three different UV intensities (5, 10 and 12 W/m²) at a RH of 50% and a flow rate of 3 L/min are presented. As expected, the mass removed per unit time per unit area increased with the UV intensity. For the intensity between 5 and 10 W/m², the mass removed for m-xylene and o, p- xylene were shown to increase slightly while the mass removed for benzene, toluene and ethylbenzene showed a slight decrease.

It can be assumed that light intensity between 5 and 10 W/m² had similar effect but gave better mass removal when the light intensity was more than doubled at 12 W/m². The results of this work is agreement with that of Zhao and Yang (2003) and Strini et al. (2005) where an increase in light intensity resulted in an increase in the degradation rate of TCE and o-xylene. The decrease in m-xylene removal at intensity of 12 W/m² may be due to the UV adsorption spectrum which may not be favorable in adsorbing UV light and therefore negatively impacting its degradation (Johnson et al., 2005).

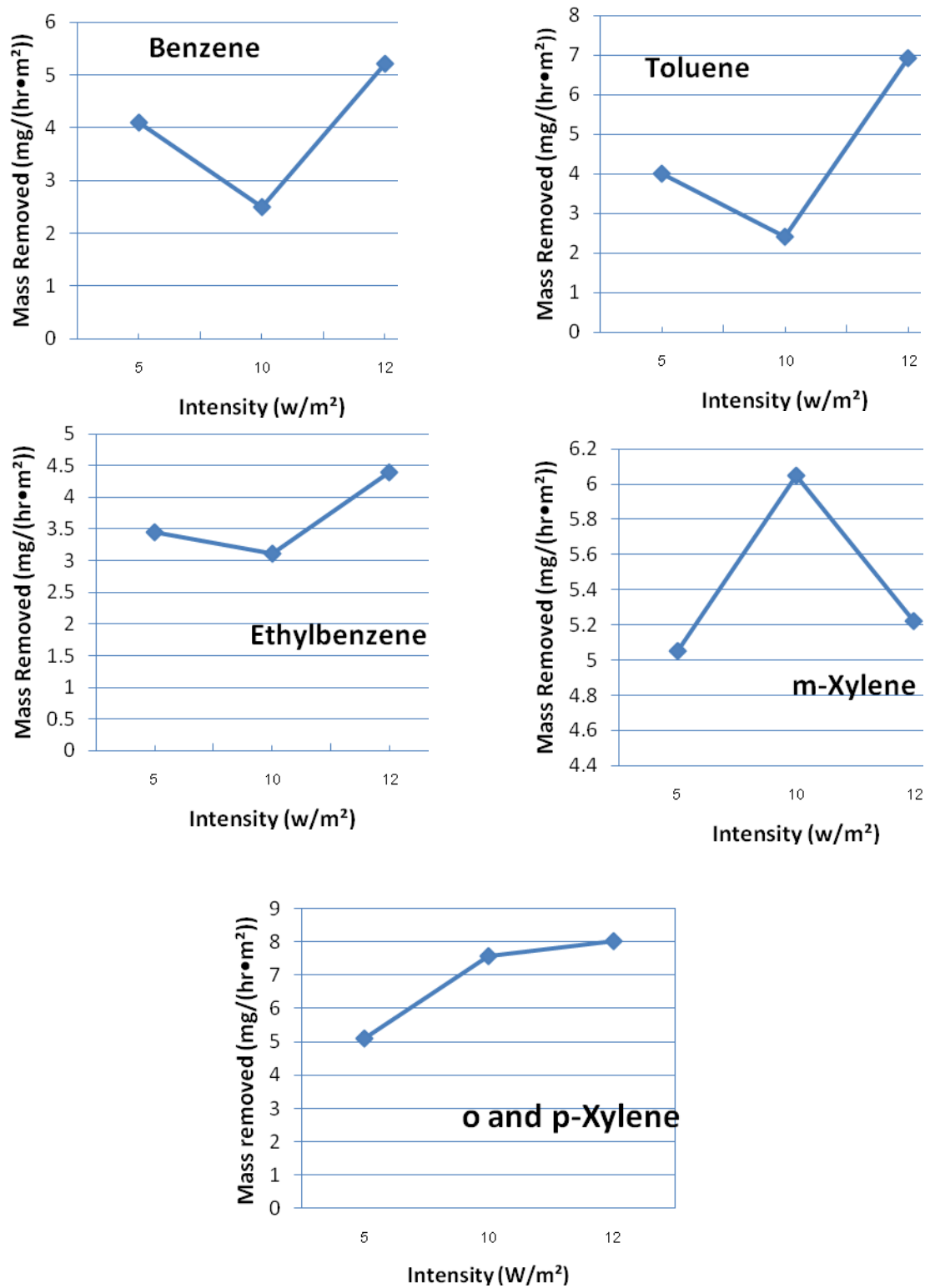


Figure 4.6 Mass of BTEX removed for different intensities

Figure 4.7 presents the data for the mass removed for different UV irradiance in one graph. The results showed that o and p-xylene were the most readily to oxidize. The order of degradation from the most difficult to oxidize to the most readily oxidized compounds was toluene > benzene > ethylbenzene > o and p-xylene which corresponded with a previous study by Strini et al. (2005).

In the case of m-xylene, the mass removed was higher with an UV intensity of 10 W/m^2 than for 12 W/m^2 .

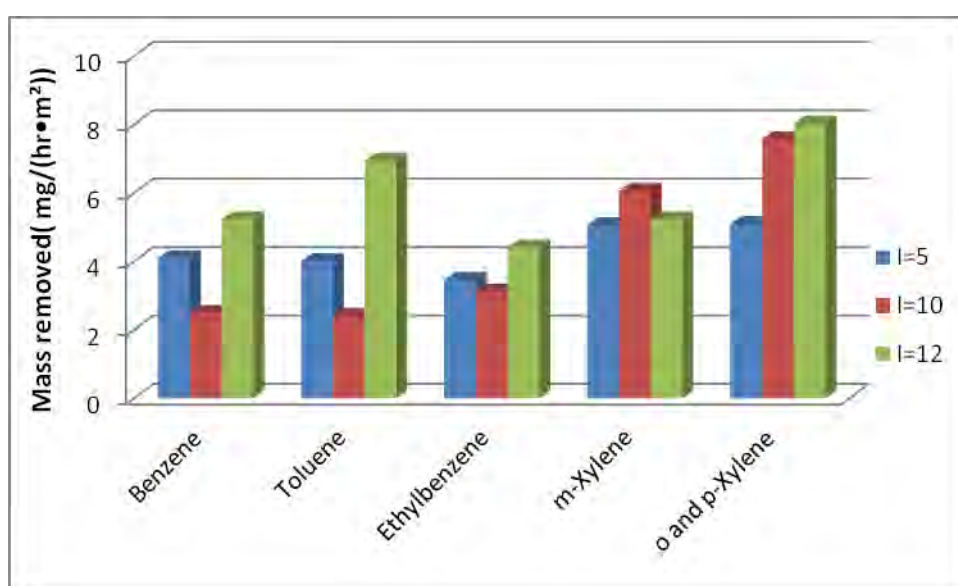


Figure 4.7 overall Mass removed of BTEX for different intensities

4.5 Effect of aging on BTEX degradation

The last set of experimental runs examined the impact of the slab at different times after they were prepared. The mass removal per time per unit area of each BTEX compound in the presence of UV light source for a freshly prepared slab (laboratory slabs), the slab one month later and the slab three months. It was presented in Fig. 4.8. The RH was set at 50%, flow rate at 3 L/min and the intensity at 10 W/m². From this data, the mass removed for ethylbenzene and m-xylene were found to decrease with the age of the slab while toluene and o, p-xylene showed a decrease from time zero to 1 month but then showed a slight increase for the slab in the third month. Based on the results, one can presume that the mass removed for one month and three months may be the same in comparison to the initial mass removed when the slab was freshly prepared. For benzene, the mass removed showed a slight increase for the 1 month slab but the mass removed for the 3 month slab was the same as the freshly prepared slab. It seemed possible that there may be a loss of active sites on surface area over time due to the generation of reaction by-products or intermediates such as calcium carbonate which may blind the catalyst surface (Blanco et al., 1996; Ollis, 2000) or the pore at catalyst surface may be blocked by the fouling (Zhao and Yang, 2003).

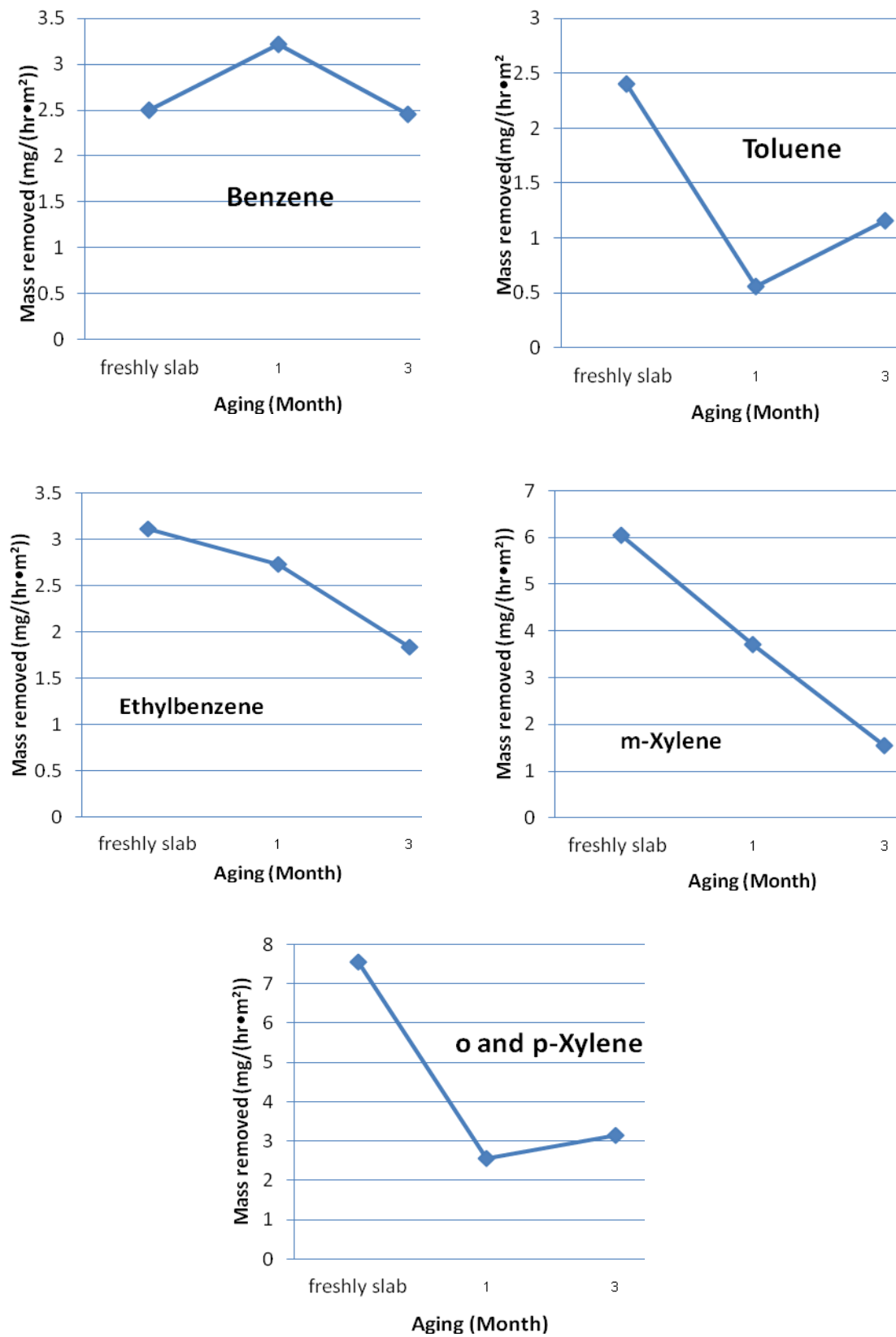


Figure 4.8 Mass of BTEX removed for slab at different times after preparati

CHAPTER V

CONCLUSIONS AND RECOMMEDATIONS

5.1 Conclusions

This study provides an account of and the reasons for the widespread use of TiO₂ –based concrete in mitigating outdoor air pollution such as benzene, toluene, ethylbenzene, m-xylene and o-, p-xylene. The study investigated the effects of relative humidity, flow rate, intensity and slab aging on BTEX degradation. Within the conditions of the present study, the main conclusions of the study are as follows:

- The optimum RH condition was found to be about 50% with lower mass removed for low RH (10%) and high RH (70%).
- Low flow rate over the slab would increase the contact time which in turn resulted in higher percent removal of BTEX. However, on a mass basis, the mass removed was lower for low flow rates.
- Mass removed for all BTEX compounds except for m-xylene were found to increase with an increase in UV intensity to 12 W/m².
- Percent removal of BTEX decrease with time and it seemed possible that the lost of removal may be due to loss of active site in the mortar slab.

The evidence presented in this study suggests that addition of TiO₂ photocatalyst to the concrete for road pavements can be used in mitigating air pollution and purifying motor vehicle pollution. This study may not answer all the questions raised by interested parties, but provides the first steps in building a body of knowledge that can be used to compare this technology with other innovative pollution purification technologies and traditional purification technologies. Actual applications will need to consider the highly variable environmental conditions and other effects such as rain and dust which may impact the effectiveness of the TiO₂-based cementitious materials.

5.2 Recommendations for Future Work

- There are other parameters that needs further study and may have an effect on the effectiveness of TiO₂- based pavement. These parameters include pollutant concentration, % of TiO₂ in slab, macro-structural characterization (porosity, surface roughness), TiO₂ coating method, TiO₂-modified cement type, and concentration of oxygen in the air.
- There is a need to understand the mechanisms and factors which lead to catalyst deactivation.
- Modelling of catalytic reactor performance should be developed for a pilot-scale practice or field work.
- There is a need in bridging the gap between artificial lab-scale and real environment conditions.
- Research should be conducted on the regeneration techniques that may be applied in-situ or in parallel configured reactor modules.
- Another research challenge is identification of reaction products and understanding of degradation pathways.

REFERENCES

- Alberici, R.M., Canela, M.C., Eberlin M.N. et al. Catalyst deactivation in the gas phase destruction of nitrogen-containing organic compounds using TiO₂/UV-VIS, Applied Catalytic B: Environmental 30 (March 2001) : 389-397.
- Ameen, M.M., and Raupp, G.B. Reversible catalyst deactivation in the photocatalytic oxidation of dilute o-xylene in air, Journal of Catalysis 184 (May 1999) : 112–122.
- Anibal, M.R., Demeestere, K., Belie, N.D., Mantyla, T., Levanen, E. 2010. Titanium dioxide coated cementitious materials for air purifying purposes: Preparation, Characterization and toluene removal potential, Building and Environment 45 (April 2010) : 832-838.
- Ao, C.H., Lee, S.C., Mak, C.L., Chan, L.Y. Photodegradation of volatile organic compounds (VOCs) and NO for indoor air purification using TiO₂: promotion versus inhibition effect of NO, Applied Catalysis B: Environmental 42 (May 2003) : 119-129.
- Ao, C.H., Lee, S.C. Enhancement effect of TiO₂ immobilized on activated carbon filter for the photodegradation of pollutants at typical indoor air level, Applied Catalytic B: Environmental 44 (August 2003) : 191-205.
- Ao, C.H.; Lee, S.C.; Yu, J.Z.; and Xu, J.H. Photodegradation of formaldehyd by photocatalyst TiO₂: effects on the presences of NO, SO₂ and VOCs, Applied Catalysis B: Environmental 54 (November 2004) : 41-50.
- Ballari, M.M., Yu, Q.L., Brouwers, H.J.H. Experimental study of the NO and NO₂ degradation by photocatalytically active concrete, Catalysis Today 161 (March 2011) : 175-180.
- Beeldens, A. An environmental friendly solution for air purification and self-cleaning effect: the application of TiO₂ as photocatalyst in concrete, Belgian Road Research Centre. Proceedings of Transport Research Arena, Europe - TRA, Göteborg, Sweden, June, 2006.

- Beeldens, A. Air purification by road materials: results of the test project in Antwerp. In: Baglioni P, Cassar L, eds. RILEM Int. On photocatalysis, environment and construction materials, Italy (October 2007) : 187–194.
- Belver, C., L'opez-Muñoz, M.J., Coronado, J.M., Soria, J. Palladium enhanced resistance to deactivation of titanium dioxide during the photocatalytic oxidation of toluene vapors, Applied Catalysis B: Environment 46 (February 2003) : 497–509.
- Berdahl, P., and H. Akbari. Evaluation of Titanium Dioxide as a Photocatalyst for Removing Air Pollutants, pp.7-9. California Energy Commission, PIER Energy-Related Environmental Research Program. CEC-500-2007-112, 2008.
- Blanco, J., Avila, P., Bahamonde, A., Alvaraz, E., Sanchez, B., Romero, M. Photocatalytic destruction of toluene and xylene at gas phase on a titania based monolithic catalyst, Catalysis Today 29 (May 1996) : 437-442.
- Blount, M.C., and Falconer, J.L. Steady-state surface species during toluene photocatalysis, Applied Catalysis B: Environment 39 (November 2002) : 39–50.
- Calvert, J.G. Chemistry for the 21st Century. The Chemistry of the Atmosphere: Its Impact on Global Change, pp.81-108. Blackwell Scientific Publications, Oxford, UK, 1994
- Cao, L., Gao, Z., Suib, S.L., Obee, T.N., Hay, S.O., Freihaut, J.D. Photocatalytic oxidation of toluene on nanoscale TiO₂ catalysts: Studies of deactivation and regeneration, Journal Catalysis 196 (December 2000) : 253–261.
- Cassar, L., and Pepe, C. Hydraulic binder and cement compositions containing photocatalyst particles, in: W.I.P. Organization (Ed.), Patent Cooperation Treaty, C04B 22/06. ITALCEMENTI S.p.A. , Bergamo (IT), 1998.
- Cassar L. Photocatalysis of cementitious materials: Clean buildings and clean air. Mrs Bulletin 29 (May 2004) : 328-331.
- Cassar, L., Beeldens, A., Pimpinelli, N., Guerrini, GL. Photocatalysis of cementitious materials. Proceedings International RILEM Symposium on Photocatalysis, Environment and Construction Materials. Florence, Italy (October 2007) : 131–145.

- Chen, H., Namdeo, A., and Bell, M. Classification of road traffic and roadside pollution concentrations for assessment of personal exposure, Environmental Modeling and Software 23 (March 2008) : 282-287.
- Chen, J., and Poon, C.S. Photocatalytic activity of titanium dioxide modified concretematerials – Influence of utilizing recycled glass cullets as aggregates, Environmental Science and Technology 43 (November 2009) : 8948-8952.
- Christos, A.K., Constantine, J., Stavros, G.P. The effect of water presence on the photocatalytic oxidation of Benzene, toluene, ethylbenzene and m-xylene in the gas phase, Atmospheric Environment 45 (December 2011) : 7089-7095.
- Cocheo, C., Sacco, P., Zaratini, L. Assessment of Human Exposure to Air Pollution, Encyclopedia of Environmental Health (2011) : 230–237.
- Debabrata, C. and Shimanti, D. Visible light induced photocatalytic degradation of organic pollutants, Journal of Photochemistry and Photobiology C: Photochemistry Reviews 6 (October 2005) : 186–205.
- Dechakiatkrai, C., Chen, J., Lynam, C., Wallace, G.G., Panichphant, S. Photocatalytic oxidation of methanol using titanium dioxide/single-walled carbon nanotube composite, Journal of Electrochemistry Society 154 (May 2007) : 407-411.
- Demeestere, K., De Visscher, A., Dewulf, J., Van Leeuwen, M., and Van Langenhove, H. A. New kinetic model for titanium dioxide mediated heterogeneous photocatalytic degradation of trichloroethylene in gas-phase, Applied Catalysis B: Environment 54 (December 2004) : 261–274.
- Demeestere, K., Dewulf, J., Herman, V.L. Heterogeneous Photocatalysis as an Advanced Oxidation Process for the Abatement of Chlorinated, Monocyclic Aromatic and Sulfurous Volatile Organic Compounds in Air: State of the Art, pp. 45-56, Taylor and Francis, London, UK, 2007.
- Demeestere, K., Dewulf, J., De Witte, B., Beeldens, A., Herman, V.L. 2008. Heterogeneous photocatalytic removal of toluene from air on building materials enriched with TiO₂, Building and Environment 43 (April 2008) : 406-414.

- Dylla, H., Hassan, M., Mohammad, L., Rupnow, T. and Wright, E. Evaluation of Environmental Effectiveness of Titanium Dioxide Photocatalyst Coating for Concrete Pavement, Transportation Research Record: Journal of the transportation Research Board 2164 (May 22) : 46-51.
- Dylla, H., Hassan, M. M., Schmitt, M., Rupnow, T., & Mohammad, L. N. Laboratory Investigation of the Effect of Mixed Nitrogen Dioxide and Nitrogen Oxide Gases on Titanium Dioxide Photocatalytic Efficiency in Concrete Pavements, Journal of Materials in Civil Engineering 23 (November 2011) : 1087-1093.
- Einaga, H., Futamura, S., and Ibusuki, T. Photocatalytic decomposition of benzene over TiO₂ in a humidified airstream, Physic Chemistry 1 (October 1999) : 4903–4908.
- Einaga, H., Futamura, S., and Ibusuki, T. Complete oxidation of benzene in gas phase by platinized titania photocatalysts, Environmental Science and Technology 35 (October 2001) : 1880–1884.
- Einaga, H., Futamura, S., and Ibusuki, T. Heterogeneous photocatalytic oxidation of benzene, toluene, cyclohexene and cyclohexane in humidified air: Comparison of decomposition behaviour on photoirradiated TiO₂ catalysts, Applied Catalysis B: Environmental 38 (September 2002) : 215–225.
- Environment Canada. Action on climate change and air pollution [online]. 2007.
Avaliable from :
http://www.ec.gc.ca/doc/media/m_124/brochure/BR_c1_eng.htm.
- Fujishima, A., and Zhang, X. Titanium dioxide photocatalysis: present situation and future approaches, The Comptes rendus Chimie 9 (November 2006) : 750-760.
- Guo, T., Zhipeng, B., Can, W., Tan, Z. Influence of relative humidity on the photocatalytic oxidation (PCO) of toluene by TiO₂ loaded on activated carbon fibers: PCO rate and intermediates accumulation, Applied catalysis B: Environmental 79 (February 2008) : 171-178.
- Guerrini, G.L; and Peccati, E. Photocatalytic cementitious roads for depollution, In: Baglioni P, pp. 179-186. Cassar L, eds. RILEM Int. Symp. On photocatalysis, environmental and construction materials, Italy, 2007.

- Hager, S., Bauer, R., and Kudielka, G. Photocatalytic oxidation of gaseous chlorinated organic over titanium dioxide, Chemosphere 41 (October 2000) : 1219–1225.
- Hassan, M.M., Dylla, H., Mohammad L., and Rupnow T. 2010. Evaluation of the durability of titanium dioxide photocatalyst coating for concrete pavement, Journal of Construction and Building Material 24 (August 2010) : 1456-1461.
- Hennezel, O., and Ollis, D.F. Trichloroethylene-promoted photocatalytic oxidation of air contaminants, Journal of Catalysis 167 (April 1997) : 118-126.
- Hung, W.C., Fu, S.H., Tseng, J.J., et al. Study on photocatalytic degradation of gaseous dichloromethane using pure and iron ion-doped TiO₂ prepared by the sol-gel method, Chemosphere 66 (February 2007) : 2142-2151.
- Husken, G; Hunger, M; Brouwers, H. Comparative study on cementitious products containing titanium dioxide as photo-catalyst. In: Baglioni P, pp. 147–154. Cassar L, eds. RILEM Int. Symp. On Photocatalysis, environment and construction materials. Italy, 2007.
- Husken, G.; Hunger, M.; and Brouwers, H.J.H. Experimental study of photocatalytic concrete products for air purification, Building and Environment 44 (December 2009) : 2463-2474.
- International Organization for Standardization, ISO 22197-1, Fine Ceramics (Advanced Ceramics, Advanced Technical Ceramics) Test Method for Air Purification Performance of Semiconducting Photocatalytic Materials – Part 1: Removal of Nitric Oxide, pp.1-12. International Organization for Standardization, Geneva, Switzerland, 2007.
- Ishihara, H., Koga, H., Kitaoka, T., Wariishi, H., Tomoda, A., Suzuki, R. Paperstructured catalyst for catalytic NO_x removal from combustion exhaust gas, Chemical Engineering Science 65 (May 2010) : 208-213.
- Japanese Industrial Standard (JIS), Fine ceramics (advanced ceramics, advanced technical ceramics) – Test method for air purification performance of photocatalytic materials- Part 1: Removal of nitric oxide, pp. 1-9. Japanese Standards Association, Tokyo, Japan, 2004.

- Jimenez, J.L, Koplow, M.D., Nelson, D.D., Zahniser, M.S., and Schmidt, S.E. Characterization of on-road vehicle NO emissions by a TILDAS remote sensor, Journal of Air and Waste Management Association 49 (December 1999) : 463-470.
- Johnson, J.T., Stephen, C.H., James, D.M., Raymond, D.H. Characterization of cancer risk from airborne benzene exposure, Regulatory Toxicology and Pharmacology 55 (December 2009) : 361–366.
- Jun, T.S., Kang, G.M., Wi, S.Y. Paint composition for antibiosis and VOCs removal, pp.3-4. Korea Published Patent Application. KR2001100052-A, 2001.
- Juyoung, J., Kazuhiko, S., Wookeun, L., Kazuhiko, S. 2005. Photodegradation of gaseous volatile organic compounds (VOCs) using TiO₂ photoirradiated by an ozone-producing UV lamp: decomposition characteristics, identification of by-products and water-soluble organic intermediates, Journal of photochemistry and photobiology A: Chemistry 169 (April 2005) : 279-287.
- Kirman, C.R., Grant, R.L. Quantitative human health risk assessment for 1,3 butadiene based upon ovarian effects in rodents, Regulatory Toxicology and Pharmacology 62 (March 2012) : 371–384.
- Ku, Y., Ma, C.M., and Shen, Y.S. Decomposition of gaseous trichloroethylene in a photoreactor with TiO₂-coated nonwoven fiber textile, Applied Catalysis B: Environmental 34 (November 2001) : 181–190.
- Kuhns, H.D., Mazzoleni, C., Moosmuller, H., Nikolic, D., Keislar, R.E., Barber, P.W., Li, Z., Etyemezian, V., Watson, J.G. Remote sensing of PM, NO, CO, HC emission factors for on-road gasoline and diesel engine vehicles in Las Vegas, NV, Science of the Total Environment 322 (April 2004) : 123-137.
- Lackhoff, M., Prieto, X., Nestle, N., et al. Photocatalytic activity of semiconductor-modified cement influence of semiconductor type and cement aging, Applied Catalysis B: Environmental 43 (July 2003) : 205-216.
- Liu, H., Cheng, S., Zhang, J., Cao, C., and Jiang, W. The gas-photocatalytic degradation of trichloroethylene without water, Chemosphere 35 (December 1997) : 2881–2889.

- Liu, T., Li, F.B., Li, X.Z. TiO₂ hydrosols with high activity for photocatalytic degradation of formaldehyde in a gaseous phase, Journal of Hazardous Material 152 (March 2008) : 347-355.
- Maggos, T; Plassais, A; Bartzis, J.G; Vasilakos, C; Moussiopoulos, N; Bonafous, L. Photocatalytic degradation of NO_x in a pilot street canyon configuration using TiO₂ – mortar panel, Environmental Monitoring and Assessment 1369 (July 2007) : 35-44.
- Martra, G., Coluccia, S., Marchese, L., Augugliaro, V., Loddo, V., Palmisano, L., and Schiavello, M. The role of H₂O in the photocatalytic oxidation of toluene in vapour phase on anatase TiO₂ catalyst: A FTIR study, Catalysis Today 53 (November 1999) : 695–702.
- McConnell, R., Islam, T., Shankardass, K., Jerrett, M., Lurmann, F., Gilliland, F., Gauderman, J., Avol, E., Kuenzli, N., Yao, L., Peters, J., and Berhane, K. Childhood incident asthma and traffic-related air pollution at home and school, pp.1-33. National Institute of Environmental Health Sciences, 2010.
- Mcharry, J. Stress and the environment: the impact of motor vehicles, Human stress and the environment : health aspects, pp. 34-49. Yverdon, Switzerland, 1994.
- Mo, J., Zhang, Y., Q., Zhu, Y., Lamson, J.J., Zhao, R. Determination and risk assessment of by-products resulting from photocatalytic oxidation of toluene, Applied Catalysis B: Environmental 89 (July 2009) : 570-576.
- Murata, Y., Tawara, H., Obata, H., Takeuchi, K. Air purifying pavement: development of photocatalytic concrete blocks, Journal of Advanced Oxidation Technologies 4 (July 1999) : 227–230.
- Ollis, D.F. Photocatalytic purification and remediation of contaminated air and water. Comptes Rendus De L Acedemie Des Sciences Serie Ii Fascicule C-Chimie 3 (November 2000) : 405-411.
- Panya, W. Control strategy for mobile source in Thailand [online]. 1997. Pollution Control Department (PCD), http://aqnis.pcd.go.th/webfm_send/1007.
- Photocatalytic Innovative Coverings Applications for Depollution Assessment, PICADA. Report for Supply Network, GROWTH project GRD1-2001-40449, PICADA, Brussels, Belgium, 2006.

- Poon, C.S., and Cheung, E. Performance of photocatalytic paving blocks made from waste, Waste and Resource Management 159 (October 2007) : 165–171.
- Portela, R., Sanchez, B., Coronado, J. M. Photocatalytic oxidation of H₂S on TiO₂ and TiO₂-ZrO₂ thin films, Journal of Advance Oxidizing Technology 10 (May 2007) : 375-380.
- Quici, N., Vera, M.L., Choi, H., Puma, G.L., Dionysiou, D.D., Litter, M.I., Destailats, H. Effect of key parameters on the photocatalytic oxidation of toluene at low concentrations in air under 254 - 185 nm UV irradiation, Applied Catalysis B: Environmental 95 (April 2010) : 312-319.
- Rachel, A., Subrahmanyam, M., Boule, P. Comparison of photocatalytic efficiencies of TiO₂ in suspended and immobilized form for the photocatalytic degradation of nitrobenzenesulfonic acids, Applied Catalysis B: Environmental 37 (July 2002) : 301-308.
- Ramirez, A.M., Demeestere, K., De Belle, N., Mantyla, T., Levanen, E. Titanium dioxide coated cementitious materials for air purification purposes: Preparation, characterization and toluene removal potential, Building and Environment 45 (April 2010) : 832-838.
- Ruot, B., Plassais, A., Olive, F., Guillot, L., Bonafous, L. TiO₂-containing cement pastes and mortars: measurements of the photocatalytic efficiency using a rhodamine B-based colourimetric test, Solar Energy 83 (October 2009) : 1794–1801.
- Sawyer, R.F., Harley, R.A., Cadle, S.H., Norbeck, J.M., Slott, R., Bravo, H.A. Mobile sources critical review: 1998 NARSTO assessment, Atmospheric Environment 34 (June 2000) : 2161–2181.
- Schwartz, J. 2011. Long-Term Effects of Particulate Air Pollution on Human Health, Encyclopedia of Environmental Health (2011) : 520–527.
- Shang, G., Zhou, J., Zhao, F., et al. Sunlight controlled self cleaning glass and its producing method, pp.1-9. China Published Patent Application, CN1944310-A, 2007.
- Shen, Y.S., and Ku, Y. Decomposition of gas-phase trichloroethylene by the UV/TiO₂ process in the presence of ozone, Chemosphere 46 (July 2002) : 101–107.

- Sikkema, J.K., J.E. Alleman, S.K. Ong, J. A. Koziel, and P. C. Taylor. Photocatalytic concrete pavements: Decrease in NO_x removal due to reaction product blinding, pp.18-21, International Conference on Long-Life Concrete Pavements-2012, Seattle, Washington, 2012.
- Simons, P.Y., and Dachille, F. The structure of TiO₂II, a high-pressure phase of TiO₂, Acta Crystallographica 23 (April 1967) : 334-336.
- Sleiman, M., Conchon, P., Ferronato, C., Chovelon, J.M. Photocatalytic oxidation of toluene at indoor air levels (ppbv): Towards a better assessment of conversion, reaction intermediates and mineralization, Applied Catalysis B: Environmental 86 (March 2009) : 159-165.
- Strini, A., Cassese, S., and Schiavi. L. Measurement of benzene, toluene, ethylbenzene and *o*-xylene gas phase photodegradation by titanium dioxide dispersed in cementitious materials using a mixed flow reactor, Applied Catalysis B: Environmental 61 (October 2005) : 90–97.
- Takeuchi, M., Deguchi, J., Sakai, S., Anpo, M. Effect of H₂O vapor addition on the photocatalytic oxidation of ethanol, acetaldehyde and acetic acid in the gas phase on TiO₂ semiconductor powders, Applied Catalysis B: Environmental 96 (April 2010) : 218-223.
- Tao, Z., Hewings, G., and Kieran, D. An economic analysis of Midwestern US criteria pollutant emissions trends from 1970 to 2000, Ecological Economic 69 (June 2010) : 1666-1674.
- Thoma, E.D., Shores, R.C., Isakov, V., Baldauf, R.W. Characterization of near road pollutant gradients using path-integrated optical remote sensing, Journal of the Air & waste Management Association 58 (July 2008) : 879-890.
- United States Environmental Protection Agency (EPA), EPA 400-F-92-00, Air toxics from motor vehicles [online]. 1995. Available from : <http://www.epa.gov/oms/consumer/02-toxic.pdf> [2012, September 22]
- United States Environmental Protection Agency (EPA). Environmental Protection Agency Primary National Ambient Air Quality Standard for Sulfur Dioxide 75 (June 2010) : 35520-35603.

- United States Environmental Protection Agency (EPA), Nitrogen Dioxide: Health [online]. 2011. Available from :
<http://www.epa.gov/air/nitrogenoxides/health.html> [2012, October 10]
- Wang, H., Wang, J., Yang, F. Antifogging self-cleaning glass and preparation method, China Published Patent Application, CN1872758-A, 2006.
- Wang, H.Q., Wu, Z.B., Zhao, W.R., et al. Photocatalytic oxidation of nitrogen oxides using TiO₂ loading on woven glass fabric, Chemosphere 66 (January 2007) : 185-190.
- Wang, S., Ang, H.M., Tade, M.O. 2007. Volatile organic compounds in indoor environment and photocatalytic oxidation: state of the art, Environment International 33 (July 2007) : 694-705.
- Wang, J.X., Chen, C.Y., Liu, Y., Jiao, F., Li, W., Lao, F., et al. Potential neurological lesion after nasal instillation of TiO₂ nanoparticles in the anatase and rutile crystal phases, Toxicology Letters 183 (December 2008) : 72–80.
- Wu, Z.B., Gu, Z.L, Zhao, W.R., et al. Photocatalytic oxidation of gaseous benzene over nanosized TiO₂ prepared by solvothermal method, China Science Bulletin 55 (November 2007) : 3601-3067.
- Yu, C.M. Deactivation and regeneration of environmentally exposed titanium dioxide (TiO₂) based products, pp.3-21. Environmental Protection Department, HKSAR, Department Order Reference Number: E183413, 2003.
- Zhang, Y.P, Yang, R., Zhao, R.Y. A model for analyzing the performance of photocatalytic air cleaner in removing volatile organic compounds, Atmospheric Environment 37 (August 2003) : 3395-3399.
- Zhao, J., and Yang, X. Photocatalytic oxidation for indoor air purification: A literature review, Building and Environmental 38 (May 2003) : 645–654.

APPENDICES

Appendix A

A.1 Calibration curve for Relative humidity set

Table A.1 Calibration curve data of Benzene humidity set

Sample	Concentration (ppm)	Area
1	0.25	1936
2	0.5	3840
3	1.0	9440

$$y = 0.000110067x, R^2 = 0.969596$$

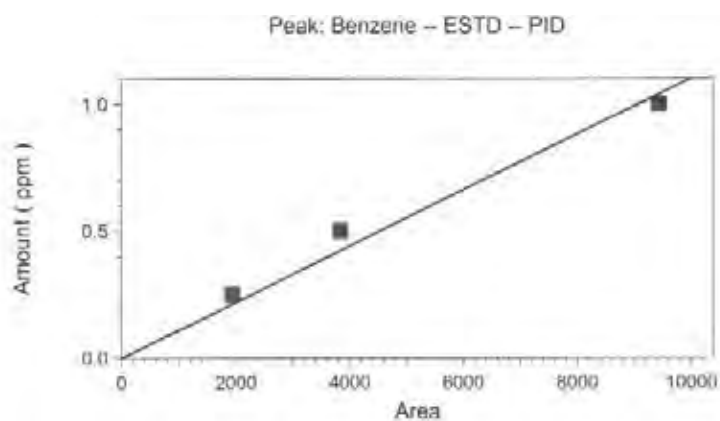


Figure A.1 Calibration curve of Benzene for RH set

Table A.2 Calibration curve data of Toluene humidity set

Sample	Concentration (ppmv)	Area
1	0.25	2472
2	0.5	4466
3	1.0	12693

$$y = 8.30483 * 10^{-5} * X, R^2 = 0.925952$$

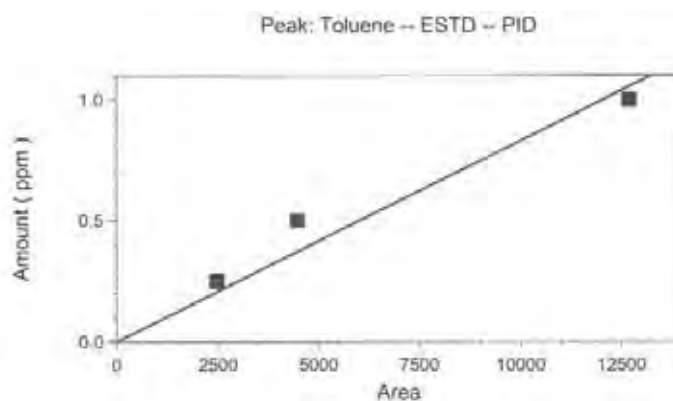


Figure A.2 Calibration curve of Toluene for RH set

Table A.3 Calibration curve data of Ethylbenzene humidity set

Sample	Concentration (ppm)	Area
1	0.25	2893
2	0.5	5870
3	1.0	15336

$$y = 6.83199 \times 10^{-5} * X, R^2 = 0.949207$$

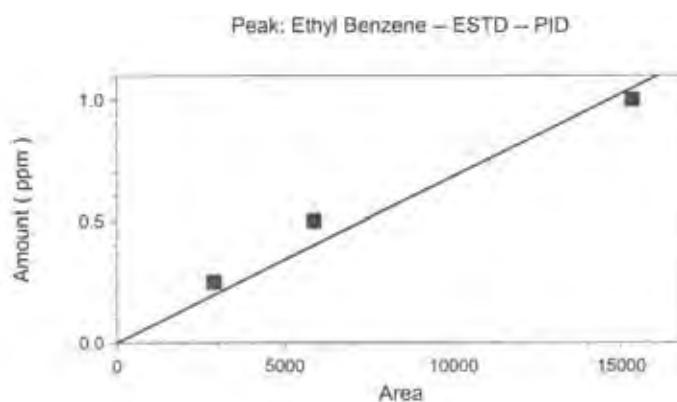


Figure A.3 Calibration curve of Ethylbenzene for RH set

Table A.4 Calibration curve data of m-Xylene humidity set

Sample	Concentration (ppm)	Area
1	0.25	1764
2	0.5	2749
3	1.0	5144

$$y = 0.000187439x, R^2 = 0.972506$$

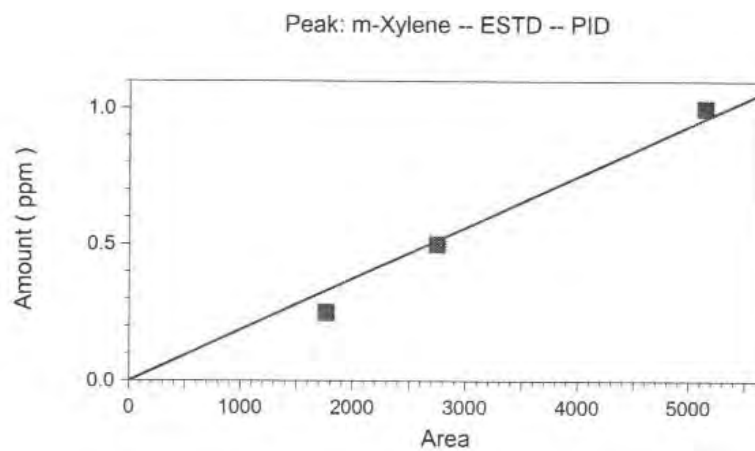


Figure A.4 Calibration curve of m-Xylene for RH set

Table A.5 Calibration curve data of o and p-Xylene humidity set

Sample	Concentration (ppm)	Area
1	0.25	2622
2	0.5	4562
3	1.0	10066

$$y = 0.000201572x, R^2 = 0.993036$$

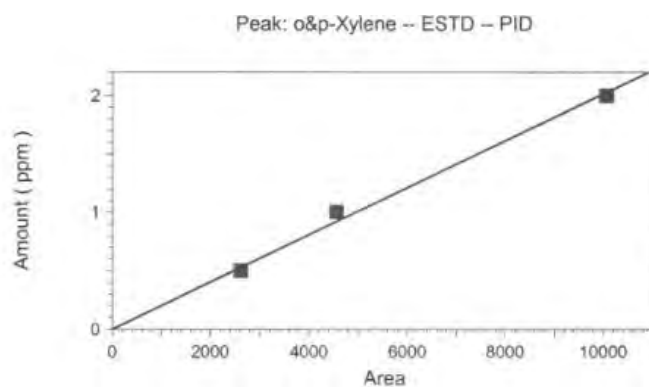


Figure A.5 Calibration curve of o and p-Xylene for RH set

A.2 Calibration curve for flow rate set

Table A.6 Calibration curve data of Benzene for flow rate set

Sample	Concentration (ppm)	Area
1	0.25	1457
2	0.5	4749
3	1.0	7150

$$y = 0.000130461x, R^2 = 0.923197$$

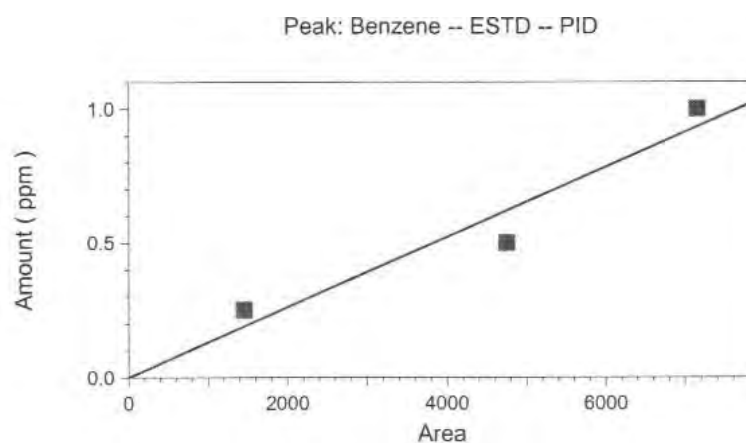


Figure A.6 Calibration curve of o and Benzene for flow rate set

Table A.7 Calibration curve data of Toluene for flow rate set

Sample	Concentration (ppm)	Area
1	0.25	2078
2	0.5	7593
3	1.0	10033

$$y = 8.82294 * 10^{-5} * X, R^2 = 0.840585$$

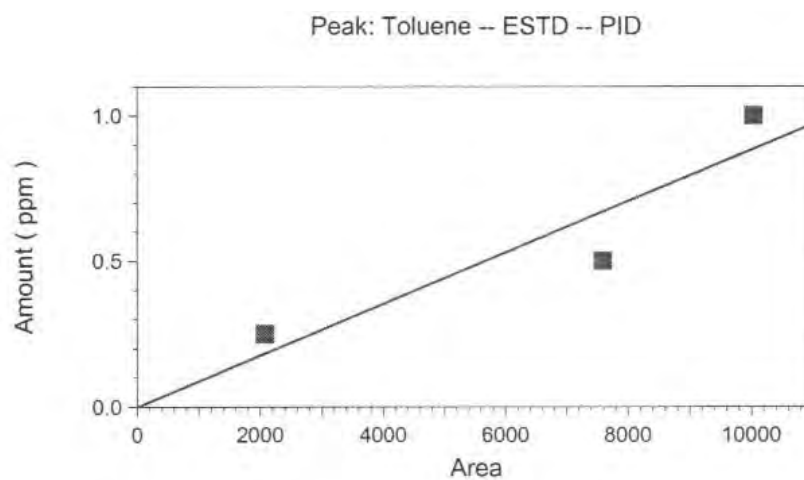


Figure A.7 Calibration curve of o and Toluene for flow rate set

Table A.8 Calibration curve data of Ethylbenzene for flow rate set

Sample	Concentration (ppm)	Area
1	0.25	2828
2	0.5	10689
3	1.0	12908

$$y = 6.56336 * 10^{-5} * X, R^2 = 0.766447$$

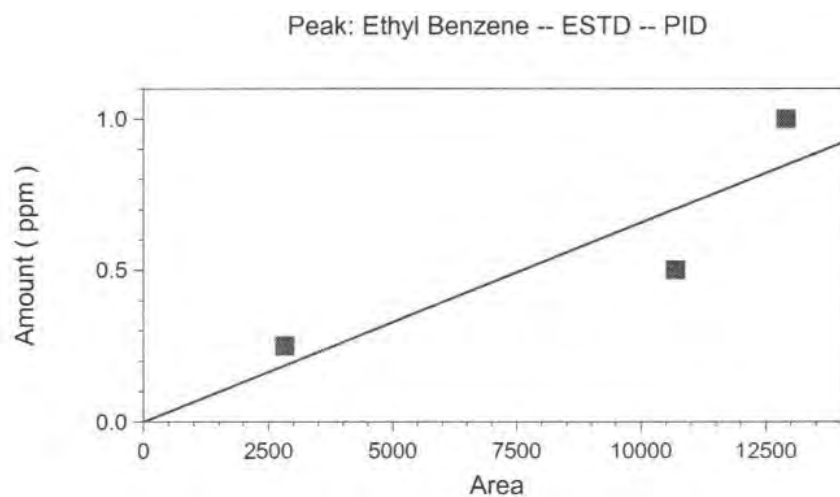
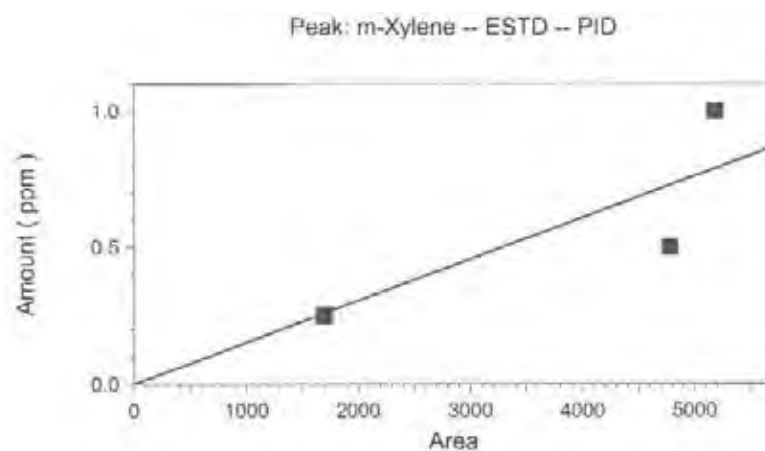


Figure A.8 Calibration curve of Ethylbenzene for flow rate set

Table A.9 Calibration curve data of m-Xylene for flow rate set

Sample	Concentration (ppm)	Area
1	0.25	1695
2	0.5	4775
3	1.0	5182

$$y = 000152175x, R^2 = 0.670415$$

**Figure A.9** Calibration curve of m-Xylene for flow rate set**Table A.10** Calibration curve data of o and p-Xylene for flow rate set

Sample	Concentration (ppm)	Area
1	0.25	2168
2	0.5	7557
3	1.0	8414

$$y = 000192068x, R^2 = 0.692961$$

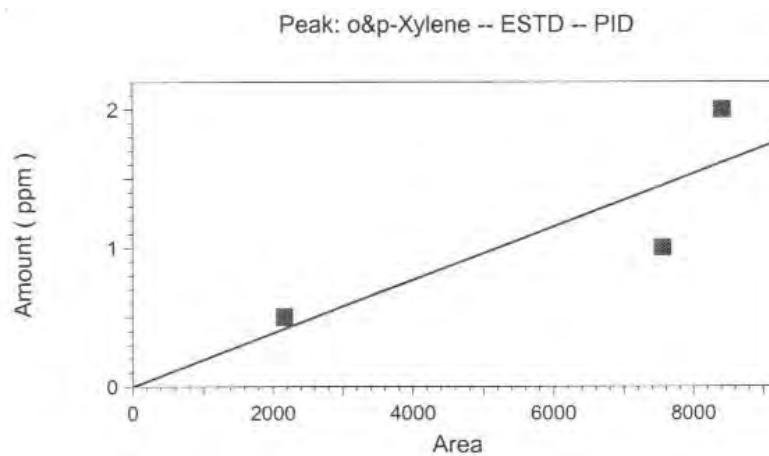


Figure A.10 Calibration curve of o and p-Xylene for flow rate set

A.3 Calibration curve for Intensity and aging set

Table A.11 Calibration curve data of Benzene for intensity and aging set

Sample	Concentration (ppm)	Area
1	0.25	2061
2	0.5	4117
3	1.0	7012

$$y = 000136288x, R^2 = 0.977188$$

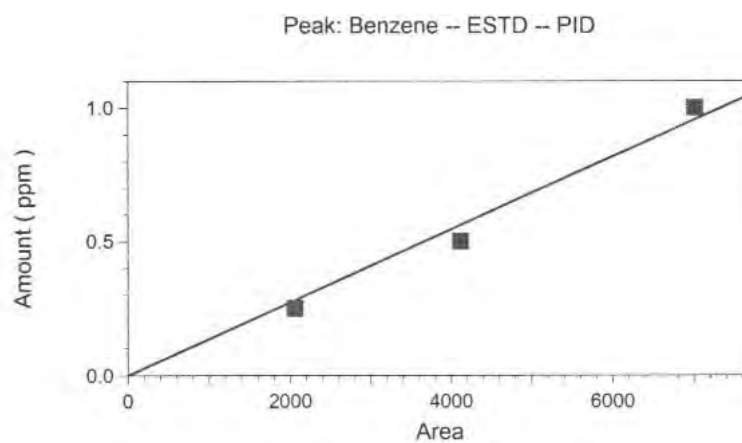
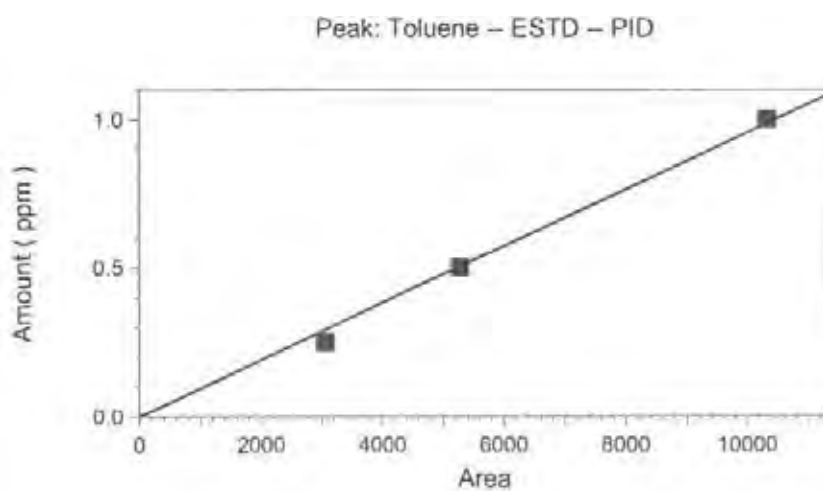


Figure A.11 Calibration curve of Benzene for flow rate set

Table A.12 Calibration curve data of Toluene for intensity and aging set

Sample	Concentration (ppm)	Area
1	0.25	3053
2	0.5	5280
3	1.0	10325

$$y = 9.54645 * 10^{-5} * X, R^2 = 0.993348$$

**Figure A.12** Calibration curve of Toluene for intensity and aging set**Table A.13** Calibration curve data of Ethylbenzene for intensity and aging set

Sample	Concentration (ppm)	Area
1	0.25	6629
2	0.5	10522
3	1.0	16285

$$y = 5.52646 * 10^{-5} * X, R^2 = 0.896520$$

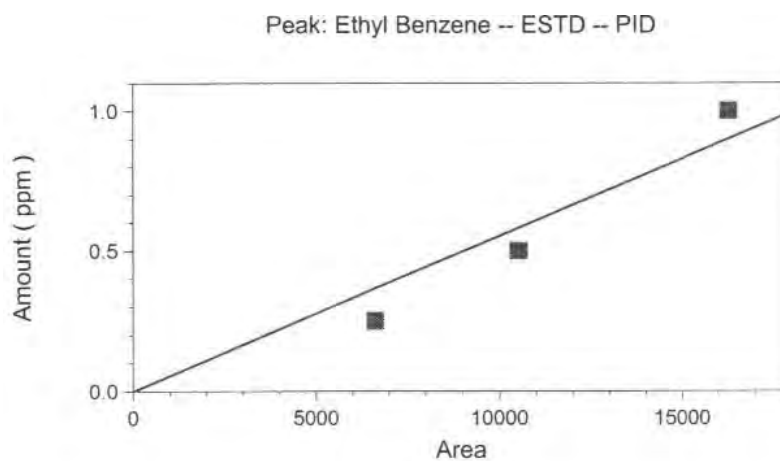
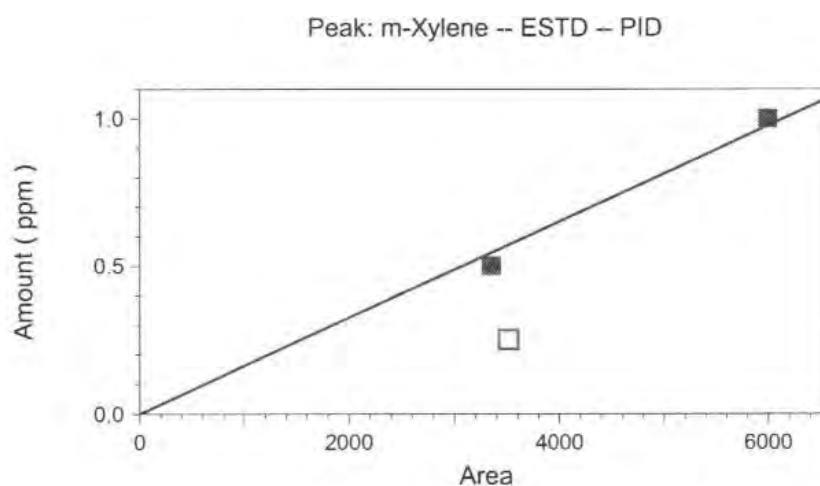


Figure A.13 Calibration curve of Ethylbenzene for intensity and aging set

Table A.14 Calibration curve data of m-Xylene for intensity and aging set

Sample	Concentration (ppm)	Area
1	0.5	3351
2	1.0	5998

$$y = 0.000162556x, R^2 = 0.979002$$



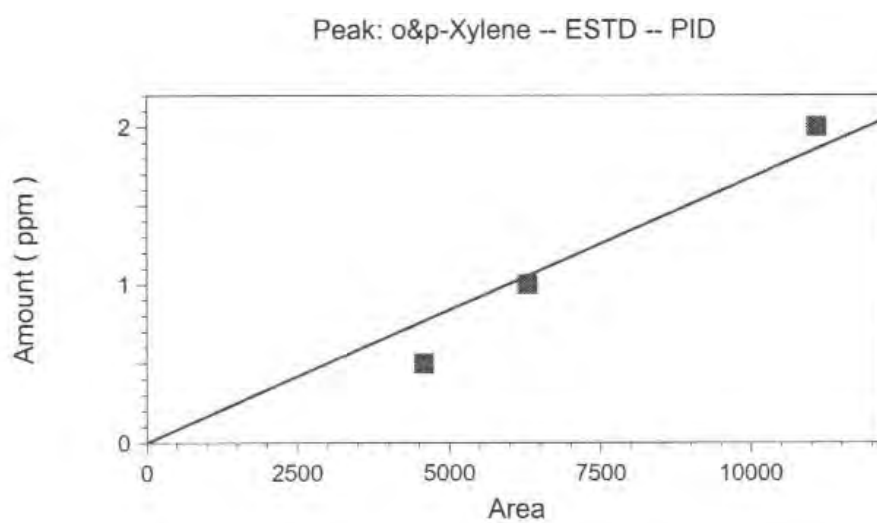
Remark: Standard gas concentration 0.25 ppm was ignored due to it was an error

Figure A.14 Calibration curve of m-Xylene for intensity and aging set

Table A.15 Calibration curve data of o and p-Xylene for intensity and aging set

Sample	Concentration (ppm)	Area
1	0.25	4581
2	0.5	6286
3	1.0	11089

$$y = 0.000167631x, R^2 = 0.918925$$

**Figure A.15** Calibration curve of o and p-Xylene for intensity and aging set

Appendix B

B.1 Mass removed and percent removal

To evaluate the results, the mass removed per time per unit surface area [$\text{mg}/(\text{hr}\cdot\text{m}^2)$] of each BTEX compound in the presence of UV light source was calculated as presented in Equations (1) and (2)

$$\text{Flow rate (m}^3/\text{hr)} \times \text{Concentrations (mg/m}^3) = \text{mg/hr} \quad (1)$$

$$\frac{\text{mg/hr}}{\text{surface area (m}^2)} = \text{mg}/(\text{hr}\cdot\text{m}^2) \quad (2)$$

To evaluate the BTEX percent removal, Equation (3) is used as follows:

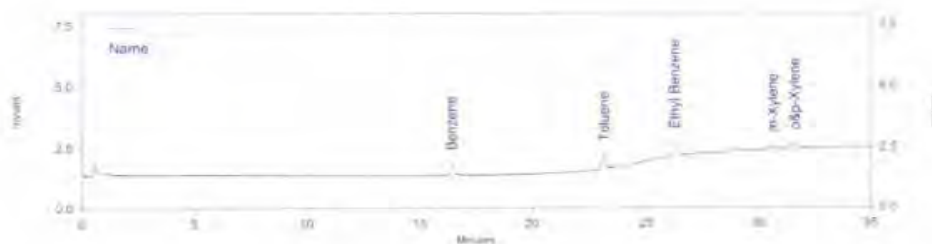
$$\text{Percent removal} = \frac{(A_0 - A_t)}{A_0} \times 100\% \quad (3)$$

Where; A_0 = Initial GC peak area of each BTEX compounds
 A_t = GC peak area of BTEX after passing the photoreactor

External Standard Report

Page 1 of 1

Method Name: C:\ASLProjects\Control\Method\btex gas .met
 Data: C:\ASLProjects\Control\Data\sample1-0130
 User: eerl
 Acquired: 1/30/2013 12:31:54 AM
 Printed: 5/6/2013 11:44:18 AM



PID Results

PK#	Name	Retention time	Area	Concentration
1	Benzene	16.447	5673	0.773
2	Toluene	23.125	5979	0.571
3	Ethyl Benzene	26.273	7149	0.395
4	m-Xylene	30.663	2532	0.412
5	o&p-Xylene	31.646	4565	0.765

Totals			25898	2.916
--------	--	--	-------	-------

Figure B.1 Chromatogram for control experiment in the bypass mode without TiO_2

External Standard Report

Page 1 of 1

Method Name: C:\ASLProjects\Control\Method\btex gas .met
 Data: C:\ASLProjects\Control\Data\sample2-0130
 User: eerl
 Acquired: 1/30/2013 1:12:36 AM
 Printed: 5/6/2013 11:44:18 AM



PID Results

PK#	Name	Retention time	Area	Concentration
1	Benzene	16.435	5890	0.768
2	Toluene	23.117	6442	0.568
3	Ethyl Benzene	26.267	5972	0.392
4	m-Xylene	30.640	2672	0.407
5	o&p-Xylene	31.605	3948	0.758

Totals			24924	2.893
--------	--	--	-------	-------

Figure B.2 Chromatogram for control experiment in the photoreactor mode without TiO_2

External Standard Report

Page 1 of 1

Method Name: C:\ASLProjects\Control\Method\btex gas .met
 Data: C:\ASLProjects\Control\Data\sample3-0130
 User: eerl
 Acquired: 1/30/2013 1:57:55 AM
 Printed: 5/6/2013 11:44:18 AM



PID Results

PK#	Name	Retention time	Area	Concentration
1	Benzene	16.327	6831	0.931
2	Toluene	23.084	7548	0.721
3	Ethyl Benzene	26.235	8880	0.491
4	m-Xylene	30.620	2881	0.414
5	o&p-Xylene	31.585	6459	1.083
Totals			32599	3.638

Figure B.3 Chromatogram for control experiment in the bypass mode without UV source

External Standard Report

Page 1 of 1

Method Name: C:\ASLProjects\Control\Method\btex gas .met
 Data: C:\ASLProjects\Control\Data\sample4-0130
 User: eerl
 Acquired: 1/30/2013 2:42:18 AM
 Printed: 5/6/2013 2:44:18 PM



PID Results

PK#	Name	Retention time	Area	Concentration
1	Benzene	16.256	7100	0.926
2	Toluene	23.055	8118	0.716
3	Ethyl Benzene	26.213	7389	0.485
4	m-Xylene	30.581	2701	0.411
5	o&p-Xylene	31.503	5595	1.075
Totals			30903	3.613

Figure B.4 Chromatogram for control experiment in the photoreactor mode without UV source

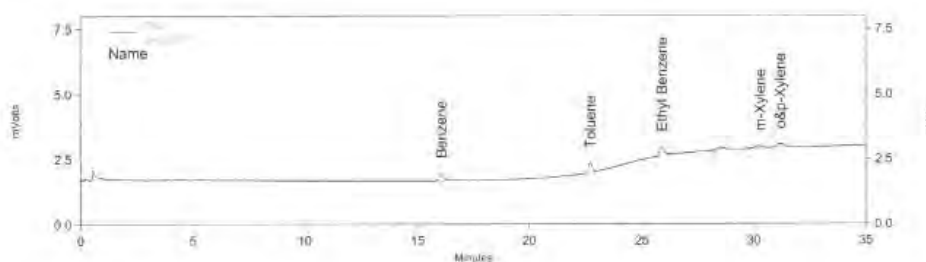
Table B.1 control experiment for No-TiO₂ and No-UV at Q=3 L/min,
RH=10%, I=10 W/m²

POLLUTANTS	No-TiO ₂		No-UV	
	CONCENTRATION (mg/L) BY PASS	CONCENTRATION (mg/L) PHOTOREACTOR	CONCENTRATION (mg/L) BY PASS	CONCENTRATION (mg/L) PHOTOREACTOR
Benzene	0.773	0.768	0.931	0.926
Toluene	0.571	0.568	0.721	0.716
Ethylbenzene	0.395	0.392	0.491	0.485
m-Xylene	0.412	0.407	0.414	0.411
o and p-Xylene	0.765	0.758	1.083	1.075

External Standard Report

Page 1 of 1

Method Name: C:\ASLProjects\BTEX\Method\btx gas 0128.met
 Data: C:\ASLProjects\BTEX\Data\sample9-0128
 User: eerl
 Acquired: 1/28/2013 10:16:51 PM
 Printed: 1/30/2013 12:07:40 PM



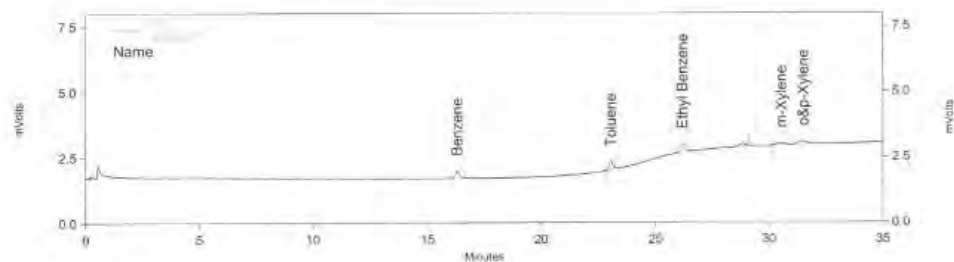
PID Results				
Pk #	Name	Retention Time	Area	Concentration
1	Benzene	16.069	3992	0.439
2	Toluene	22.730	4284	0.356
3	Ethyl Benzene	25.892	5405	0.369
5	m-Xylene	30.283	2144	0.402
6	o&p-Xylene	31.180	3362	0.678
Totals			19187	2.244

Figure B.5 Chromatogram of BTEX at Q=3 L/min, RH=10%, I=10 W/m² in the bypass mode

External Standard Report

Page 1 of 1 (13)

Method Name: C:\ASLProjects\BTEX\Method\bftex gas 0128.met
 Data: C:\ASLProjects\BTEX\Data\sample10-0128
 User: eerl
 Acquired: 1/28/2013 11:14:09 PM
 Printed: 1/29/2013 3:19:57 PM



PID Results				
Pk #	Name	Retention Time	Area	Concentration
1	Benzene	16.314	3567	0.393
2	Toluene	23.052	3938	0.327
3	Ethyl Benzene	26.188	4454	0.304
5	m-Xylene	30.538	2079	0.390
6	o&p-Xylene	31.513	3051	0.615
Totals			17089	2.029

Figure B.6 Chromatogram of BTEX at $Q=3$ L/min, $RH=10\%$, $I=10$ W/m² in the photoreactor mode

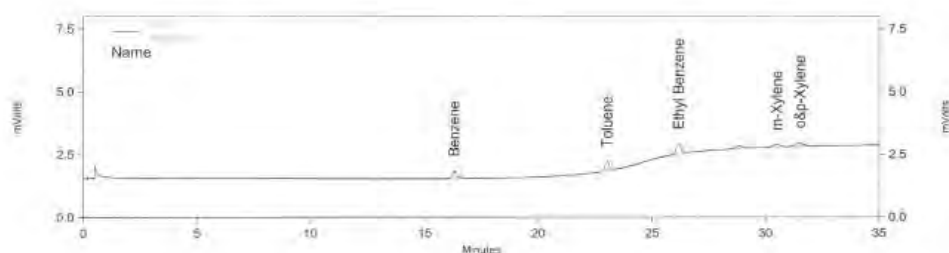
Table B.2 Mass removed of BTEX at $Q=3$ L/min, $RH=10\%$, $I=10$ W/m²

POLLUTANTS	Q=3 L/min, RH=10%, I=10 W/m ²		MASS REMOVED[mg/(hr•m ²)]
	CONCENTRATION (mg/L) BY PASS	CONCENTRATION (mg/L) PHOTOREACTOR	
Benzene	0.439	0.393	1.16
Toluene	0.356	0.327	0.86
Ethylbenzene	0.369	0.304	2.22
m-Xylene	0.402	0.39	0.41
o- and p-Xylene	0.678	0.615	2.15

External Standard Report

Page 1 of 1 (6)

Method Name: C:\ASL\Projects\BTEX\Method\btex gas 0128.met
 Data: C:\ASL\Projects\BTEX\Data/sample3-0128
 User: eerl
 Acquired: 1/28/2013 3:52:19 PM
 Printed: 1/29/2013 3:19:39 PM



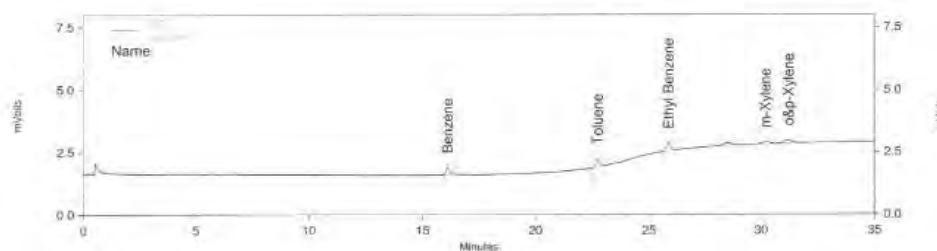
PID Results				
PK #	Name	Retention Time	Area	Concentration
1	Benzene	16.292	3698	0.407
2	Toluene	23.035	4588	0.381
3	Ethyl Benzene	26.168	5699	0.389
5	m-Xylene	30.475	2406	0.451
6	o&p-Xylene	31.505	3821	0.770
Totals			20212	2.399

Figure B.7 Chromatogram of BTEX at Q=3 L/min, RH=25%, I=10 W/m² in the bypass mode

External Standard Report

Page 1 of 1 (7)

Method Name: C:\ASL\Projects\BTEX\Method\btex gas 0128.met
 Data: C:\ASL\Projects\BTEX\Data/sample4-0128
 User: eerl
 Acquired: 1/28/2013 5:25:46 PM
 Printed: 1/29/2013 3:19:42 PM



PID Results				
PK #	Name	Retention Time	Area	Concentration
1	Benzene	16.119	3350	0.369
3	Toluene	22.747	3732	0.310
4	Ethyl Benzene	25.878	4504	0.308
6	m-Xylene	30.198	2242	0.420
7	o&p-Xylene	31.213	3219	0.649
Totals			17047	2.055

Figure B.8 Chromatogram of BTEX at Q=3 L/min, RH=25%, I=10 W/m² in the photoreactor mode

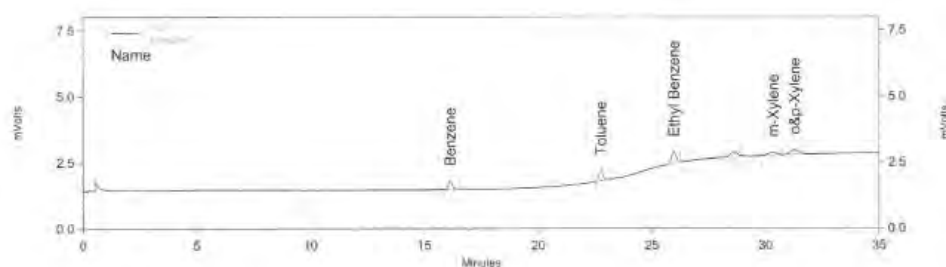
Table B.3 Mass removed of BTEX at Q=3 L/min, RH=25%, I=10 W/m²

POLLUTANTS	Q=3 L/min, RH=25%, I=10 W/m ²		MASS REMOVED[mg/(h r•m ²)]
	CONCENTRATION (mg/L) BY PASS	CONCENTRATION (mg/L) PHOTOREACTOR	
Benzene	0.407	0.369	0.96
Toluene	0.381	0.31	2.1
Ethylbenzene	0.389	0.308	2.77
m-Xylene	0.451	0.42	1.06
o- and p-Xylene	0.77	0.649	4.13

External Standard Report

Page 1 of 1 (4)

Method Name: C:\ASLProjects\BTEX\Method\btex gas 0128.met
 Data: C:\ASLProjects\BTEX\Data\sample1-0128
 User: eerl
 Acquired: 1/28/2013 1:57:25 PM
 Printed: 1/29/2013 3:19:34 PM



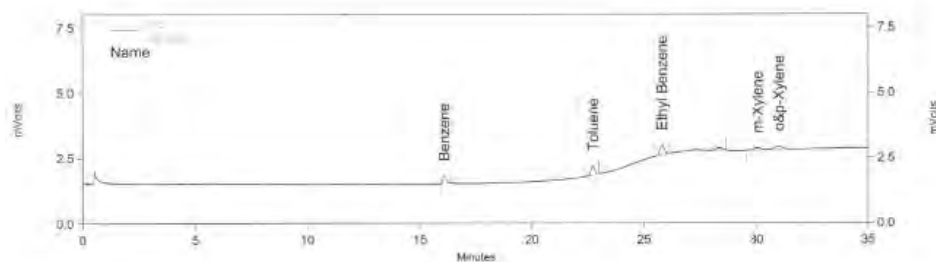
PID Results				
Pk #	Name	Retention Time	Area	Concentration
1	Benzene	16.141	4274	0.470
2	Toluene	22.769	5125	0.426
3	Ethyl Benzene	25.987	6134	0.419
5	m-Xylene	30.333	3322	0.623
6	o&p-Xylene	31.275	4294	0.866
Totals			23149	2.803

Figure B.9 Chromatogram of BTEX at Q=3 L/min, RH=50%, I=10 W/m² in the bypass mode

External Standard Report

Page 1 of 1 (5)

Method Name: C:\ASLProjects\BTEX\Method\btex gas 0128.met
 Data: C:\ASLProjects\BTEX\Data\sample2-0128
 User: eerl
 Acquired: 1/28/2013 2:56:19 PM
 Printed: 1/29/2013 3:19:37 PM



PID Results				
Pk #	Name	Retention Time	Area	Concentration
1	Benzene	16.082	3370	0.371
2	Toluene	22.744	4154	0.345
3	Ethyl Benzene	25.813	4802	0.328
5	m-Xylene	30.041	2377	0.446
6	o&p-Xylene	31.000	3201	0.645
Totals			17904	2.135

Figure B.10 Chromatogram of BTEX at Q=3 L/min, RH=50%, I=10 W/m² in the photoreactor mode

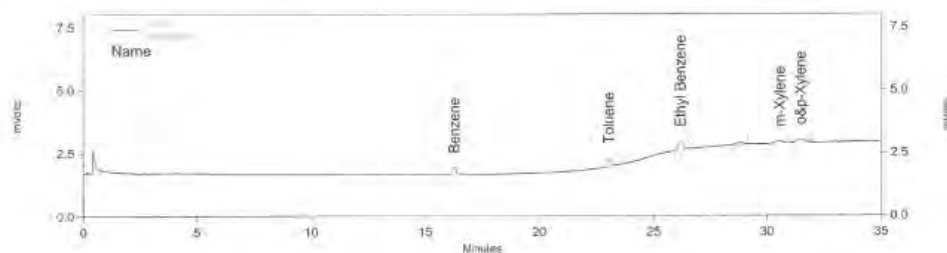
Table B.4 Mass removed of BTEX at Q=3 L/min, RH=50%, I=10 W/m²

POLLUTANTS	Q=3 L/min, RH=50%, I=10 W/m ²		MASS REMOVED [mg/(h r•m ²)]
	CONCENTRATION (mg/L) BY PASS	CONCENTRATION (mg/L) PHOTOREACTOR	
Benzene	0.47	0.371	2.49
Toluene	0.426	0.345	2.4
Ethylbenzene	0.419	0.328	3.11
m-Xylene	0.623	0.446	6.05
o and p-Xylene	0.866	0.645	7.56

External Standard Report

Page 1 of 1

Method Name: C:\ASLProjects\BTEX\Method\btex gas 0128.met
 Data: C:\ASLProjects\BTEX\Data/sample 7-0128
 User: eerl
 Acquired: 1/28/2013 8:23:15 PM
 Printed: 1/30/2013 12:19:12 PM



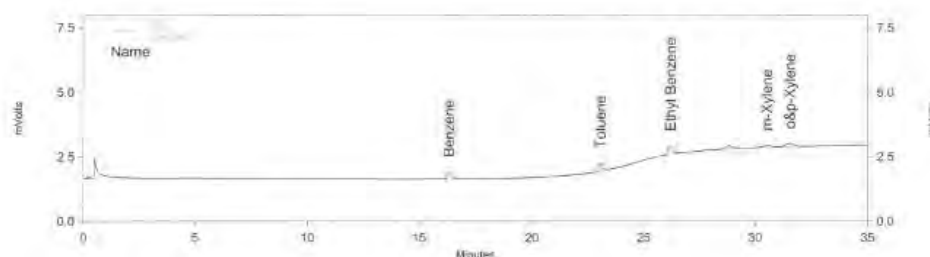
PID Results				
PK #	Name	Retention Time	Area	Concentration
1	Benzene	16.276	3680	0.405
2	Toluene	23.040	4270	0.355
3	Ethyl Benzene	26.188	5049	0.345
5	m-Xylene	30.566	2026	0.380
6	o&p-Xylene	31.476	3656	0.737
Totals			18681	2.221

Figure B.11 Chromatogram of BTEX at Q=3 L/min, RH=70%, I=10 W/m² in the bypass mode

External Standard Report

Page 1 of 1

Method Name: C:\ASLProjects\BTEX\Method\btex gas 0128.met
 Data: C:\ASLProjects\BTEX\Data/sample8-0128
 User: eerl
 Acquired: 1/28/2013 9:20:04 PM
 Printed: 1/30/2013 12:20:55 PM



PID Results				
PK #	Name	Retention Time	Area	Concentration
1	Benzene	16.334	3380	0.372
2	Toluene	23.067	3776	0.314
3	Ethyl Benzene	26.208	4544	0.310
5	m-Xylene	30.511	2022	0.379
6	o&p-Xylene	31.531	2966	0.598
Totals			16688	1.973

Figure B.12 Chromatogram of BTEX at Q=3 L/min, RH=70%, I=10 W/m² in the photoreactor mode

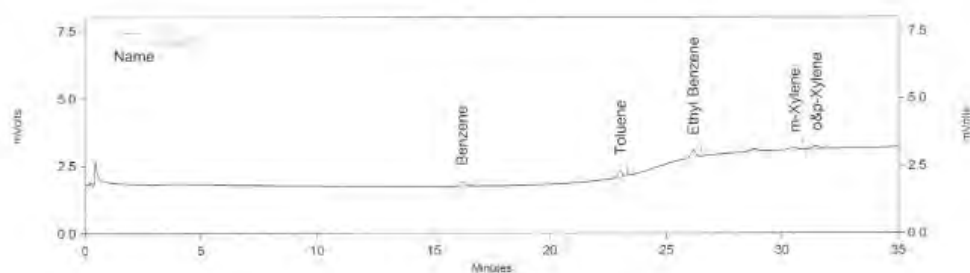
Table B.5 Mass removed of BTEX at Q=3 L/min, RH=70%, I=10 W/m²

POLLUTANTS	Q=3 L/min, RH=50%, I=10 W/m ²		MASS REMOVED [mg/(hr•m ²)]
	CONCENTRATION (mg/L) BY PASS	CONCENTRATION (mg/L) PHOTOREACTOR	
Benzene	0.405	0.372	0.78
Toluene	0.355	0.314	1.21
Ethylbenzene	0.345	0.310	1.19
m-Xylene	0.380	0.379	0.03
o and p-Xylene	0.737	0.598	4.74

External Standard Report

Page 1 of 1 (8)

Method Name: C:\ASLProjects\BTEX\Method\btex gas 0129.met
 Data: C:\ASLProjects\BTEX\Data\sample5-0129
 User: eerl
 Acquired: 1/29/2013 11:18:42 PM
 Printed: 1/30/2013 11:47:28 AM



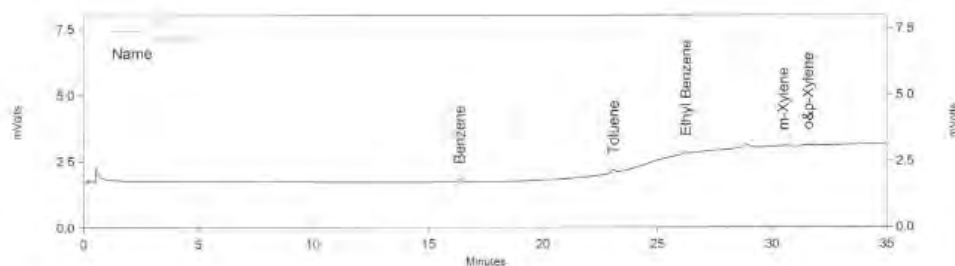
PID Results				
PK #	Name	Retention Time	Area	Concentration
1	Benzene	16.209	3245	0.423
2	Toluene	23.032	3064	0.270
3	Ethyl Benzene	26.172	3886	0.255
5	m-Xylene	30.526	1992	0.303
6	o&p-Xylene	31.476	2919	0.561
Totals			15106	1.813

Figure B.13 Chromatogram of BTEX at Q=1 L/min, RH=50%, I=10 W/m² in the bypass mode

External Standard Report

Page 1 of 1 (9)

Method Name: C:\ASLProjects\BTEX\Method\btex gas 0129.met
 Data: C:\ASLProjects\BTEX\Data\sample6-0129
 User: eer1
 Acquired: 1/30/2013 12:22:09 AM
 Printed: 1/30/2013 11:47:31 AM



PID Results				
Pl #	Name	Retention Time	Area	Concentration
1	Benzene	16.367	1226	0.160
2	Toluene	23.100	1341	0.118
3	Ethyl Benzene	26.238	1648	0.108
5	m-Xylene	30.483	1035	0.158
6	o&p-Xylene	31.560	1052	0.202
Totals			6302	0.746

Figure B.14 Chromatogram of BTEX at Q=1 L/min, RH=50%, I=10 W/m² in the photoreactor mode

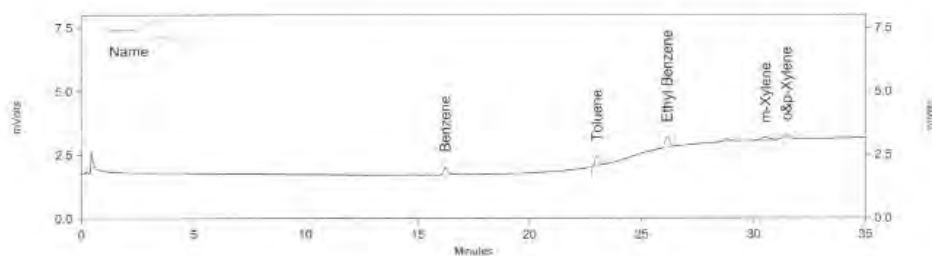
Table B.6 Mass removed of BTEX at Q=1 L/min, RH=50%, I=10 W/m²

POLLUTANTS	Q=1 L/min, RH=50%, I=10 W/m ²		MASS REMOVED[mg/(h r•m ²)]
	CONCENTRATION (mg/L) BY PASS	CONCENTRATION (mg/L) PHOTOREACTOR	
Benzene	0.423	0.160	2.2
Toluene	0.270	0.118	1.5
Ethylbenzene	0.255	0.108	1.67
m-Xylene	0.303	0.158	1.65
o- and p-Xylene	0.561	0.202	4.09

External Standard Report

Page 1 of 1 (6)

Method Name: C:\ASLProjects\BTEX\Method\btex gas 0129.met
 Data: C:\ASLProjects\BTEX\Data\sample3-0129
 User: eerl
 Acquired: 1/29/2013 9:24:20 PM
 Printed: 1/30/2013 11:47:22 AM



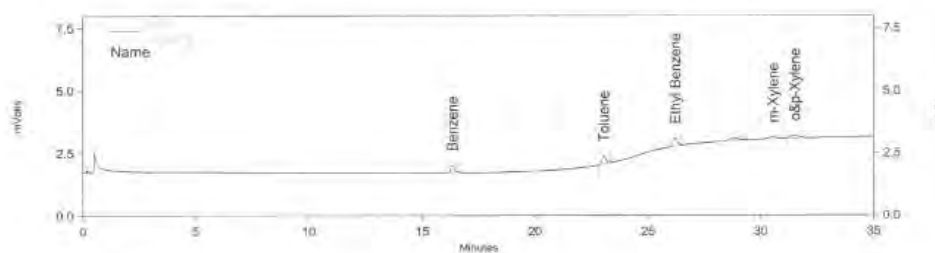
PID Results				
Pk #	Name	Retention Time	Area	Concentration
1	Benzene	16.236	4429	0.578
2	Toluene	23.027	4757	0.420
3	Ethyl Benzene	26.145	6029	0.396
5	m-Xylene	30.521	2384	0.363
6	o&p-Xylene	31.455	4020	0.772
Totals			21619	2.528

Figure B.15 Chromatogram of BTEX at Q=5 L/min, RH=50%, I=10 W/m² in the bypass mode

External Standard Report

Page 1 of 1 (7)

Method Name: C:\ASLProjects\BTEX\Method\btex gas 0129.met
 Data: C:\ASLProjects\BTEX\Data\sample4-0129
 User: eerl
 Acquired: 1/29/2013 10:23:47 PM
 Printed: 1/30/2013 11:47:25 AM



PID Results				
Pk #	Name	Retention Time	Area	Concentration
1	Benzene	16.341	3325	0.434
2	Toluene	23.055	3969	0.350
3	Ethyl Benzene	26.205	4283	0.281
5	m-Xylene	30.538	1855	0.282
6	o&p-Xylene	31.501	2838	0.545
Totals			16270	1.892

Figure B.16 Chromatogram of BTEX at Q=5 L/min, RH=50%, I=10 W/m² in the photoreactor mode

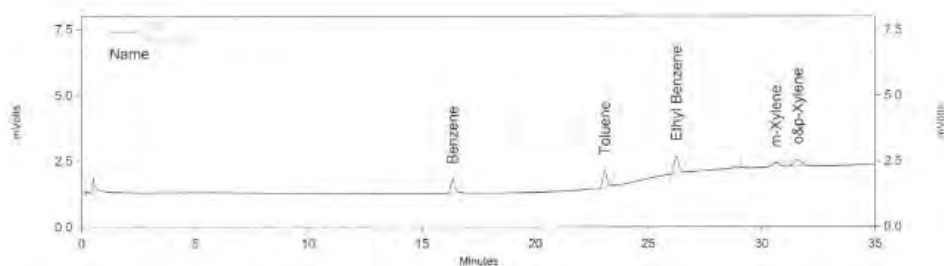
Table B.7 Mass removed of BTEX at Q=5 L/min, RH=50%, I=10 W/m²

POLLUTANTS	Q=5 L/min, RH=50%, I=10 W/m ²		MASS REMOVED[mg/(h r•m ²)]
	CONCENTRATION (mg/L) BY PASS	CONCENTRATION (mg/L) PHOTOREACTOR	
Benzene	0.578	0.434	6.03
Toluene	0.420	0.350	3.46
Ethylbenzene	0.396	0.281	6.55
m-Xylene	0.363	0.282	4.61
o and p-Xylene	0.772	0.545	12.9

External Standard Report

Page 1 of 1 (3)

Method Name: C:\ASLProjects\BTEX\Method\btex gas 0129.met
 Data: C:\ASLProjects\BTEX\Data\sample3-0207
 User: eerl
 Acquired: 2/7/2013 5:46:58 PM
 Printed: 2/8/2013 2:46:45 PM



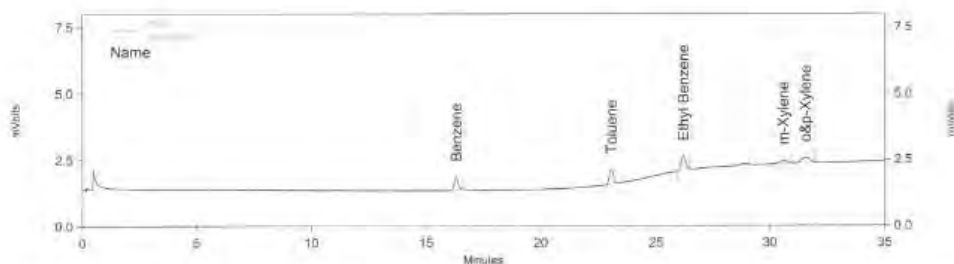
PID Results				
PK #	Name	Retention Time	Area	Concentration
1	Benzene	16.352	6729	0.917
2	Toluene	23.084	7943	0.758
3	Ethyl Benzene	26.242	9638	0.533
5	m-Xylene	30.595	3210	0.461
6	o&p-Xylene	31.568	5631	0.944
Totals			33151	3.612

Figure B.17 Chromatogram of BTEX at Q=3 L/min, RH=50%, I=5 W/m² in the bypass mode

External Standard Report

Page 1 of 1 (1)

Method Name: C:\ASLProjects\BTEX\Method\btex gas 0129.met
 Data: C:\ASLProjects\BTEX\Data\sample7-0207
 User: eerl
 Acquired: 2/7/2013 8:48:24 PM
 Printed: 2/8/2013 2:53:49 PM



PID Results				
PK #	Name	Retention Time	Area	Concentration
1	Benzene	16.329	5536	0.754
2	Toluene	23.069	6522	0.623
3	Ethyl Benzene	26.217	7247	0.401
5	m-Xylene	30.578	2603	0.374
6	o&p-Xylene	31.538	4744	0.795
Totals			26652	2.946

Figure B.18 Chromatogram of BTEX at $Q=3$ L/min, $RH=50\%$, $I=5$ W/m² in the photoreactor mode

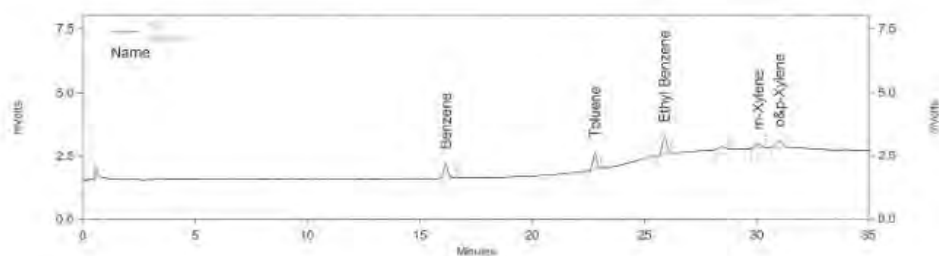
Table B.8 Mass removed of BTEX at $Q=3$ L/min, $RH=50\%$, $I=5$ W/m²

POLLUTANTS	Q=3 L/min, RH=50%, I=5 W/m ²		MASS REMOVED [mg/(h r•m ²)]
	CONCENTRATION (mg/L) BY PASS	CONCENTRATION (mg/L) PHOTOREACTOR	
Benzene	0.917	0.754	4.09
Toluene	0.758	0.623	4.00
Ethylbenzene	0.502	0.401	3.45
m-Xylene	0.522	0.374	5.05
o and p-Xylene	0.944	0.795	5.09

External Standard Report

Page 1 of 1 (1)

Method Name: C:\ASLProjects\BTEX\Method\btex gas 0129.met
 Data: C:\ASLProjects\BTEX\Data\sample1-0207
 User: eerl
 Acquired: 2/7/2013 3:55:36 PM
 Printed: 2/14/2013 10:07:03 PM



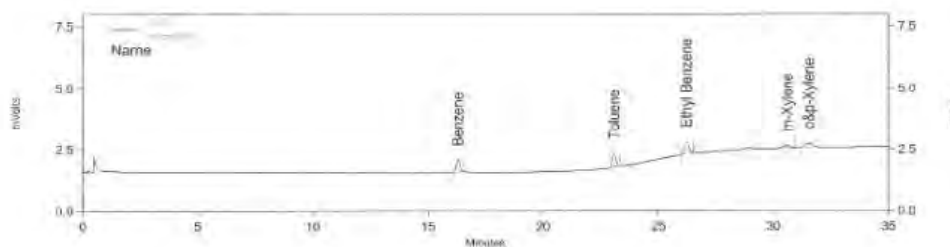
PID Results				
PK #	Name	Retention Time	Area	Concentration
1	Benzene	16.149	7480	1.019
2	Toluene	22.777	8421	0.804
3	Ethyl Benzene	25.865	9242	0.511
6	m-Xylene	30.045	3287	0.534
7	o&p-Xylene	30.991	5838	0.979
Totals			34268	3.847

Figure B.19 Chromatogram of BTEX at Q=3 L/min, RH=50%, I=12 W/m² in the bypass mode

External Standard Report

Page 1 of 1 (2)

Method Name: C:\ASLProjects\BTEX\Method\btex gas 0129.met
 Data: C:\ASLProjects\BTEX\Data\sample2-0207
 User: eerl
 Acquired: 2/7/2013 4:49:40 PM
 Printed: 2/14/2013 10:07:06 PM



PID Results				
PK #	Name	Retention Time	Area	Concentration
1	Benzene	16.302	5954	0.811
2	Toluene	23.062	5972	0.570
3	Ethyl Benzene	26.207	6910	0.382
5	m-Xylene	30.596	2346	0.381
6	o&p-Xylene	31.546	4441	0.744
Totals			25623	2.889

Figure B.20 Chromatogram of BTEX at Q=3 L/min, RH=50%, I=12 W/m² in the photoreactor mode

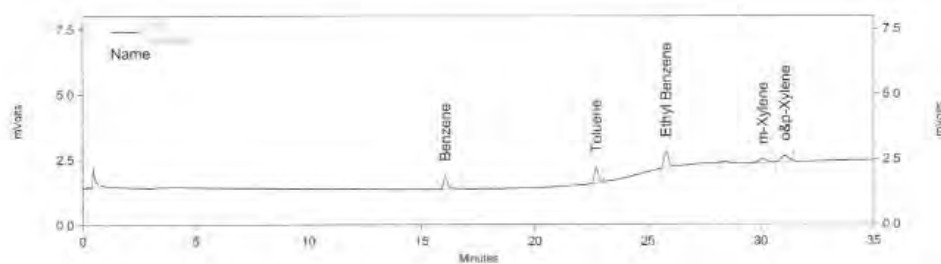
Table B.9 Mass removed of BTEX at Q=5 L/min, RH=50%, I=12 W/m²

POLLUTANTS	Q=3 L/min, RH=50%, I=12 W/m ²		MASS REMOVED[mg/(hr•m ²)]
	CONCENTRATION (mg/L) BY PASS	CONCENTRATION (mg/L) PHOTOREACTOR	
Benzene	1.019	0.811	5.22
Toluene	0.804	0.570	6.93
Ethylbenzene	0.511	0.382	4.40
m-Xylene	0.534	0.381	5.22
o and p-Xylene	0.979	0.744	8.02

External Standard Report

Page 1 of 1 (1)

Method Name: C:\ASLProjects\BTEX\Method\btex gas 0129.mel
 Data: C:\ASLProjects\BTEX\Data\sample8-0207
 User: eerl
 Acquired: 2/7/2013 9:41:52 PM
 Printed: 2/8/2013 3:01:50 PM



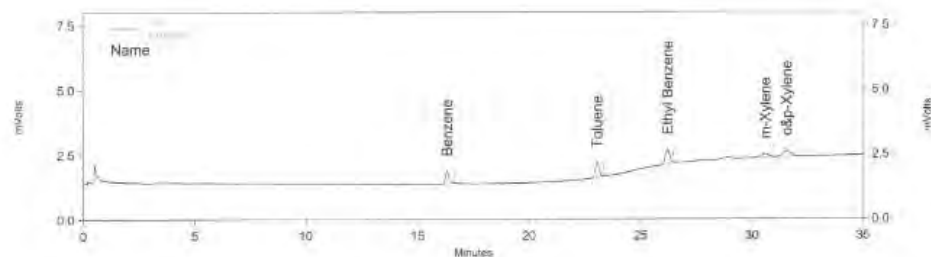
PID Results				
Pk #	Name	Retention Time	Area	Concentration
1	Benzene	16.034	6622	0.902
2	Toluene	22.730	7104	0.678
3	Ethyl Benzene	25.820	8730	0.482
5	m-Xylene	30.080	3528	0.507
6	o&p-Xylene	31.055	5514	0.924
Totals			31498	3.494

Figure B.21 Chromatogram of BTEX at Q=3 L/min, RH=50%, I=10 W/m² in the bypass mode for 1 month aging

External Standard Report

Page 1 of 1 (2)

Method Name: C:\ASLProjects\BTEX\Method\btex gas 0129.mel
 Data: C:\ASLProjects\BTEX\Data\sample9-0207
 User: eerl
 Acquired: 2/7/2013 10:37:23 PM
 Printed: 2/8/2013 3:01:52 PM



PID Results				
Pk #	Name	Retention Time	Area	Concentration
1	Benzene	16.327	5679	0.774
2	Toluene	23.075	6907	0.659
3	Ethyl Benzene	26.223	7271	0.402
4	m-Xylene	30.603	2775	0.398
5	o&p-Xylene	31.570	5063	0.849
Totals			27695	3.082

Figure B.22 Chromatogram of BTEX at Q=3 L/min, RH=50%, I=10 W/m² in the photoreactor mode for 1 month aging

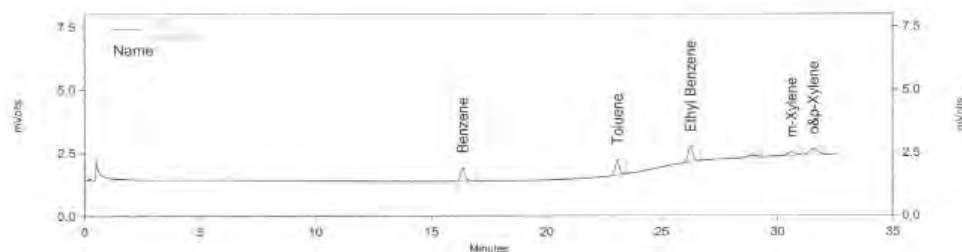
Table B.10 Mass removed of BTEX at Q=3 L/min, RH=50%, I=10 W/m² and aging 1 month

POLLUTANTS	Q=3 L/min, RH=50%, I=10 W/m ² Aging 1 month		MASS REMOVED[mg/(h r•m ²)]
	CONCENTRATION (mg/L) BY PASS	CONCENTRATION (mg/L) PHOTOREACTOR	
Benzene	0.902	0.774	3.22
Toluene	0.678	0.659	0.56
Ethylbenzene	0.482	0.402	2.73
m-Xylene	0.507	0.398	3.72
o and p-Xylene	0.924	0.849	2.56

External Standard Report

Page 1 of 1

Method Name: C:\ASLProjects\BTEX\Method\btx gas 0129.met
 Data: C:\ASLProjects\BTEX\Data\sample10-0207
 User: eerl
 Acquired: 2/7/2013 11:35:14 PM
 Printed: 2/8/2013 3:06:51 PM



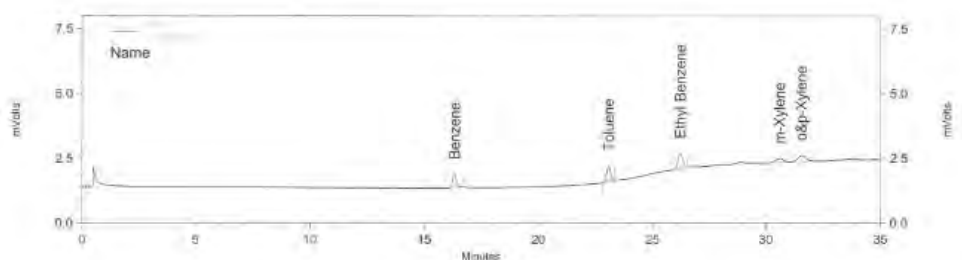
PID Results				
PK #	Name	Retention Time	Area	Concentration
1	Benzene	16.356	6959	0.948
2	Toluene	23.090	7669	0.732
3	Ethyl Benzene	26.242	9244	0.511
5	m-Xylene	30.600	3462	0.497
6	o&p-Xylene	31.555	6217	1.042
Totals			33551	3.730

Figure B.23 Chromatogram of BTEX at Q=3 L/min, RH=50%, I=10 W/m² in the bypass mode for 3 months aging

External Standard Report

Page 1 of 1 (1)

Method Name: C:\ASLProjects\BTEX\Method\btx gas 0129.met
 Data: C:\ASLProjects\BTEX\Data\sample11-0207
 User: eerl
 Acquired: 2/8/2013 12:15:53 AM
 Printed: 2/8/2013 3:06:27 PM



PID Results				
PK #	Name	Retention Time	Area	Concentration
1	Benzene	16.342	6243	0.850
2	Toluene	23.074	7263	0.693
3	Ethyl Benzene	26.232	8277	0.457
4	m-Xylene	30.585	3147	0.452
5	o&p-Xylene	31.538	5669	0.950
Totals			30599	3.403

Figure B.24 Chromatogram of BTEX at Q=3 L/min, RH=50%, I=10 W/m² in the photoreactor mode for 3 months aging

Table B.11 Mass removed of BTEX at Q=3 L/min, RH=50%, I=10 W/m² and aging 3 month

POLLUTANTS	Q=3 L/min, RH=50%, I=10 W/m ² Aging 3 month		MASS REMOVED[mg/(h r•m ²)]
	CONCENTRATION (mg/L) BY PASS	CONCENTRATION (mg/L) PHOTOREACTOR	
Benzene	0.948	0.850	2.46
Toluene	0.732	0.693	1.16
Ethylbenzene	0.511	0.457	1.84
m-Xylene	0.497	0.452	1.54
o and p-Xylene	1.042	0.95	3.14

Table B.12 Percent removal of Benzene at different flow rate

FLOW RATE	Benzene RH = 50%, I = 10 W/m ²		PERCENT REMOVAL (%)
	GC Peak Area BY PASS	GC Peak Area PHOTOREACTOR	
Q = 1 L/min	3245	1226	66.22
Q = 3 L/min	6794	5111	24.77
Q = 5 L/min	4429	3325	24.93

Table B.13 Percent removal of Toluene at different flow rate

FLOW RATE	TOLUENE RH = 50%, I = 10 W/m ²		PERCENT REMOVAL (%)
	GC Peak Area BY PASS	GC Peak Area PHOTOREACTOR	
Q = 1 L/min	3064	1341	56.23
Q = 3 L/min	7952	5721	28.06
Q = 5 L/min	4757	3969	16.57

BIOGRAPHY

NAME : Miss Tanutcha Meechaiyo

DATE OF BIRTH : 22 September 1985

PLACE OF BIRTH : Mukdahan, Thailand

HOME ADDRESS : 70/5 Wongcompa, Mukdahan, Thailand, 49000

CELL : + 66873255759

E-MAIL : meechaiyo@live.com

EDUCATION : Bachelor Degree of Environmental Engineering,
Kasetsart University.

CONFERENCE : International Conference on Environmental and
Hazardous Substance Management towards a Green
Economy (EHSM 2013)